A NOVEL UNSTRUCTURED MESH FINITE ELEMENT METHOD FOR SOLVING THE TIME-SPACE FRACTIONAL WAVE EQUATION ON A TWO-DIMENSIONAL IRREGULAR CONVEX DOMAIN

Wenping Fan [1], Fawang Liu [2], Xiaoyun Jiang [3], Ian Turner [4]

Abstract

Most existing research on applying the finite element method to discretize space fractional operators is studied on regular domains using either uniform structured triangular meshes, or quadrilateral meshes. Since many practical problems involve irregular convex domains, such as the human brain or heart, which are difficult to partition well with a structured mesh, the existing finite element method using the structured mesh is less efficient. Research on the finite element method using a completely unstructured mesh on an irregular domain is of great significance. In this paper, a novel unstructured mesh finite element method is developed for solving the time-space fractional wave equation on a two-dimensional irregular convex domain. The novel unstructured mesh Galerkin finite element method is used to discretize in space and the Crank-Nicolson scheme is used to discretize the Caputo time frational derivative. The implementation of the unstructured mesh Crank-Nicolson Galerkin method (CNGM) is detailed and the stability and convergence of the numerical scheme are analysed. Numerical examples are presented to verify the theoretical analysis. To highlight the ability of the proposed unstructured mesh Galerkin finite element method, a comparison of the unstructured mesh with the structured mesh in the implementation of the numerical scheme is conducted. The proposed numerical method using an unstructured mesh is shown to be more effective and feasible for practical applications involving irregular convex domains.

MSC 2010: Primary 26A33; Secondary 65M06, 65M12, 65M15, 35R11

Key Words and Phrases: two-dimensional time-space fractional wave equation, finite element method, unstructured mesh, irregular domain

pp. xxx–xxx, DOI: .....

1. **Introduction**

In recent years, fractional calculus has attracted great attention as a useful approach for modelling a range of anomalous transport phenomena due to its excellent performance in describing phenomena and processes with memory and hereditary properties. Fractional differential equations have been widely used to model important applications in various fields, such as physics, chemistry, biology, polymer rheology, viscoelastic materials, and control theory [22, 17, 1, 18, 21]. With the rapid development of fractional calculus, extensive research has been carried out on the implementation of efficient numerical methods, including the finite difference [11, 26, 5, 25, 15], the finite element [13, 19, 29], the finite volume [12, 16], and spectral methods [30, 26].

The finite element method has been demonstrated to be a useful numerical tool for solving fractional differential equations involving space fractional operators. Zhao et al. [28] considered the finite element method for two-dimensional space-fractional advection-dispersion equations. Zhuang et al. [32] proposed two numerical methods for a new one-dimensional space-fractional Boussinesq equation based on the finite volume and finite element methods, respectively. Choi et al. [6] studied the finite element solutions for a one-dimensional space fractional diffusion equation with a nonlinear source term. Bu et al. [3] considered a class of two-dimensional space and time fractional Bloch-Torrey equations with the time fractional derivative order defined between 0 and 1 using the finite element method implemented on a structured mesh. Zhu et al. [31] considered a fully discrete finite element method for the two-dimensional nonlinear Fisher' equation with Riesz fractional derivatives in space.

However, most existing research on applying the finite element method to fractional PDEs is studied on regular domains using either uniform structured triangular meshes, or quadrilateral meshes. Since many practical problems involve irregular convex domains, such as the simulation of biological processes evolving in the human brain or heart, research on the finite element method using a completely unstructured mesh on an irregular domain is of great significance.

In this paper, we consider the two-dimensional time-space fractional wave equation on an irregular convex domain Ω:

$$\begin{cases} {}_0^C D_t^\gamma u = K_x \frac{\partial^{2\alpha} u}{\partial |x|^{2\alpha}} + K_y \frac{\partial^{2\beta} u}{\partial |y|^{2\beta}} + f(x,y,t), \quad (x,y,t) \in \Omega \times (0,T], \\ u(x,y,0) = \psi_0(x,y), \quad (x,y) \in \Omega, \\ u_t(x,y,0) = \psi_1(x,y), \quad (x,y) \in \Omega, \\ u(x,y,t) = 0, \quad (x,y,t) \in \partial\Omega \times (0,T], \end{cases} \tag{1.1}$$

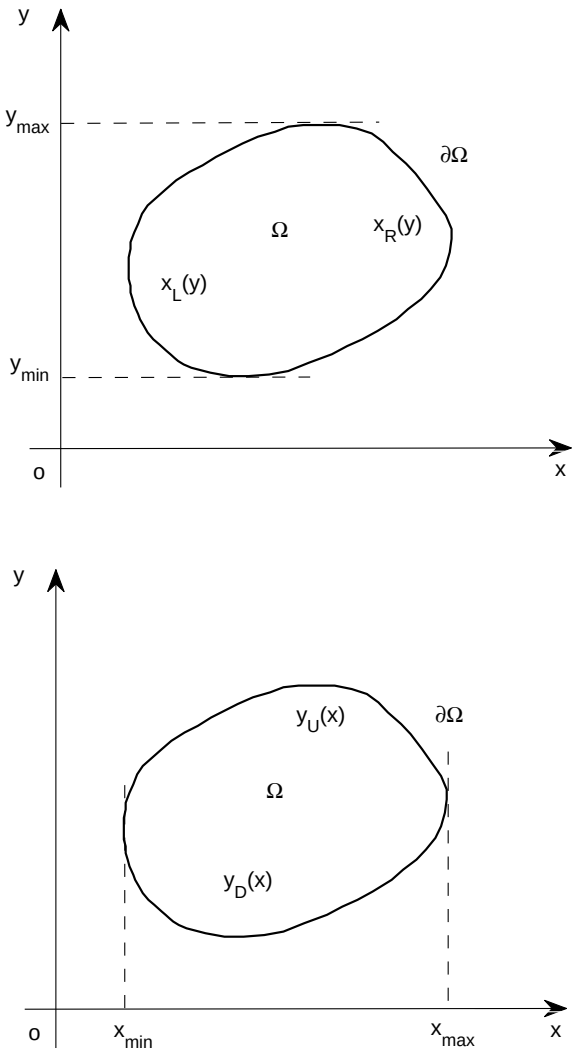

FIGURE 1.1. A convex domain Ω with boundaries $x_L(y), x_R(y), y_D(x), y_U(x)$.

where $1 < \gamma < 2$, $1/2 < \alpha, \beta < 1$, $K_x > 0, K_y > 0$. As shown in Fig. 1.1, an irregular convex domain Ω is defined as $\Omega = \{(x, y)|x_L(y) \leq x \leq x_R(y), y_D(x) \leq y \leq y_U(x)\}$, where $x_L(y), x_R(y)$ are the left and right boundaries of Ω, and $y_D(x), y_U(x)$ are the lower and upper boundaries of Ω. The time fractional derivative is defined in the Caputo sense

$$ {}_0^C D_t^\gamma u = \frac{1}{\Gamma(n-\gamma)} \int_0^t (t-s)^{n-1-\gamma} \left(\frac{d}{ds}\right)^n u(x,y,s) ds,\ n-1<\gamma<n, n\in\mathbb{N}. \tag{1.2} $$

The Riesz space fractional derivatives $\frac{\partial^{2\alpha} u}{\partial |x|^{2\alpha}}$ and $\frac{\partial^{2\beta} u}{\partial |y|^{2\beta}}$ are defined [20] by

$$ \frac{\partial^{2\alpha} u(x,y)}{\partial |x|^{2\alpha}} = -c_\alpha \Big({}_x D_L^{2\alpha} u(x,y) + {}_x D_R^{2\alpha} u(x,y) \Big), \tag{1.3} $$

$$ \frac{\partial^{2\beta} u(x,y)}{\partial |y|^{2\beta}} = -c_\beta \left({}_y D_D^{2\beta} u(x,y) + {}_y D_U^{2\beta} u(x,y) \right), \tag{1.4} $$

where $c_\alpha = \frac{1}{2\cos(\alpha\pi)}, c_\beta = \frac{1}{2\cos(\beta\pi)}$, and the Riemann-Liouville fractional derivative operators with $n-1<\mu<n$ are defined as

$$ {}_x D_L^\mu u(x,y) = \frac{1}{\Gamma(n-\mu)} \frac{\partial^n}{\partial x^n} \int_{x_L(y)}^x (x-s)^{n-\mu-1} u(s,y) ds, \tag{1.5} $$

$$ {}_x D_R^\mu u(x,y) = \frac{(-1)^n}{\Gamma(n-\mu)} \frac{\partial^n}{\partial x^n} \int_x^{x_R(y)} (s-x)^{n-\mu-1} u(s,y) ds, \tag{1.6} $$

$$ {}_y D_D^\mu u(x,y) = \frac{1}{\Gamma(n-\mu)} \frac{\partial^n}{\partial y^n} \int_{y_D(x)}^y (y-s)^{n-\mu-1} u(x,s) ds, \tag{1.7} $$

$$ {}_y D_U^\mu u(x,y) = \frac{(-1)^n}{\Gamma(n-\mu)} \frac{\partial^n}{\partial y^n} \int_y^{y_U(x)} (s-y)^{n-\mu-1} u(x,s) ds. \tag{1.8} $$

The existing finite element method used to discretize space fractional operators is designed for regular domains, such as $\Omega = [a,b]\times[c,d]$, where a, b, c, d are constants. Using a structured mesh to partition the regular domain, the nodes and elements in the partition can be numbered according to a certain law. Then, the elements in the partition can be divided into two kinds, one is the odd elements, and the other is the even elements. As a result, the computation of the fractional derivative operators can also be divided into two similar cases, one to treat the odd elements and the other to treat the even elements [3]. By optimising the numerical algorithm to take advantage of the structured property of the mesh, the implementation of the numerical scheme can be efficient and easy.

However, different from the regular domain, an irregular domain will have more complex boundaries, and it is difficult to partition well using a structured mesh. In view of this, an unstructured mesh will be much more efficient in the implementation of the finite element method for solving fractional partial differential equations on irregular domains. As a direct result of the non-regular locations of the nodes and elements in the unstructured partition, the implementation of the numerical method will be much more challenging. For the finite element method using an unstructured mesh,

the existing finite element scheme using a structured mesh is invalid. The main contribution of this research is to develop a new discretization procedure using the finite element method intended for use on both regular and irregular domains.

Hence, in this paper, a novel unstructured mesh finite element method is derived for solving the two-dimensional time-space fractional wave equation (1.1) defined on an irregular convex domain. The Crank-Nicolson method is used for the temporal discretization. To discretize in space, the Galerkin finite element method using a completely unstructured mesh is applied. The stability and convergence of the numerical scheme are discussed. To verify the theoretical analysis, two numerical examples on different convex domains are studied. Furthermore, to highlight the ability of the unstructured mesh compared with the structured mesh in the implementation of the numerical scheme, a comparison of the accuracy and the computational cost between the two kinds of partition is studied.

The rest of this paper is organized as follows. In Section 2, some definitions and lemmas are given. In Section 3, the Crank-Nicolson Galerkin method (CNGM) for the two-dimensional time-space fractional wave equation is derived. The implementation of the numerical scheme using an unstructured mesh is detailed in Section 4. In Section 5, the stability and convergence of the numerical scheme are discussed. Finally, two numerical examples are presented in Section 6 to verify the theoretical analysis. A comparison between the structured mesh and the unstructured mesh is also studied in Section 6 to show the ability of the unstructured mesh in the implementation of the numerical scheme.

2. **Preliminaries**

In this section, we need to recall some theories that has been studied previously by Ervin and Roop [9, 10], Bu *et al.* [4, 2], and Zhu *et al.* [31]. For a convex domain $\Omega \subset \mathbb{R}^2$ shown in Fig. 1.1, resulting from its irregularity, with $x_{\min} = \min\limits_{(x,y)\in\Omega} x_L(y)$, $x_{\max} = \max\limits_{(x,y)\in\Omega} x_R(y)$, $y_{\min} = \min\limits_{(x,y)\in\Omega} y_D(x)$ and $y_{\max} = \max\limits_{(x,y)\in\Omega} y_U(x)$, we denote the inner product and L^2-norm as

$$\begin{aligned}(u,v)_{L^2(\Omega)} := \int_\Omega uv d\Omega &= \int_{y_{\min}}^{y_{\max}} \int_{x_L(y)}^{x_R(y)} u(x,y)v(x,y)dxdy, \\ &= \int_{x_{\min}}^{x_{\max}} \int_{y_D(x)}^{y_U(x)} u(x,y)v(x,y)dydx,\end{aligned} \tag{2.1}$$

$$\|u\|_{L^2(\Omega)} = ((u,u)_{L^2(\Omega)})^{1/2}. \tag{2.2}$$

Definition 2.1. ([10, 4, 31]) (Left fractional derivative space). For $\mu > 0$, we define the semi-norm

$$|u|_{J_L^\mu(\Omega)} := \left(\left\| {}_xD_L^\mu u \right\|_{L^2(\Omega)}^2 + \left\| {}_yD_D^\mu u \right\|_{L^2(\Omega)}^2 \right)^{\frac{1}{2}}, \tag{2.3}$$

and norm

$$\|u\|_{J_L^\mu(\Omega)} := \left(\|u\|_{L^2(\Omega)}^2 + |u|_{J_L^\mu(\Omega)}^2 \right)^{\frac{1}{2}}, \tag{2.4}$$

where $J_L^\mu(\Omega), J_{L,0}^\mu(\Omega)$ denote the closure of $C^\infty(\Omega), C_0^\infty(\Omega)$ with respect to $\|\cdot\|_{J_L^\mu(\Omega)}$.

Definition 2.2. ([10, 4, 31]) (Right fractional derivative space). For $\mu > 0$, we define the semi-norm

$$|u|_{J_R^\mu(\Omega)} := \left(\left\| {}_xD_R^\mu u \right\|_{L^2(\Omega)}^2 + \left\| {}_yD_U^\mu u \right\|_{L^2(\Omega)}^2 \right)^{\frac{1}{2}}, \tag{2.5}$$

and norm

$$\|u\|_{J_R^\mu(\Omega)} := \left(\|u\|_{L^2(\Omega)}^2 + |u|_{J_R^\mu(\Omega)}^2 \right)^{\frac{1}{2}}, \tag{2.6}$$

where $J_R^\mu(\Omega), J_{R,0}^\mu(\Omega)$ denote the closure of $C^\infty(\Omega), C_0^\infty(\Omega)$ with respect to $\|\cdot\|_{J_R^\mu(\Omega)}$.

Definition 2.3. ([10, 4, 31]) (Fractional Sobolev space). For $\mu > 0$, we define the semi-norm

$$|u|_{H^\mu(\Omega)} := \| |\xi|^\mu \mathcal{F}(u)(\xi) \|_{L^2(\Omega)} \tag{2.7}$$

and norm

$$\|u\|_{H^\mu(\Omega)} := \left(\|u\|_{L^2(\Omega)}^2 + |u|_{H^\mu(\Omega)}^2 \right)^{\frac{1}{2}}, \tag{2.8}$$

where $\mathcal{F}(u)(\xi)$ is the Fourier transformation of the function u, and $H^\mu(\Omega)$, $H_0^\mu(\Omega)$ denote the closure of $C^\infty(\Omega), C_0^\infty(\Omega)$ with respect to $\|\cdot\|_{H^\mu(\Omega)}$.

Definition 2.4. ([10, 4, 31]) (Symmetric fractional derivative space). For $\mu > 0, \mu \neq n - \frac{1}{2}, n \in \mathbb{N}$, we define the semi-norm

$$|u|_{J_S^\mu(\Omega)} := \left(\left| \left({}_xD_L^\mu u,\ {}_xD_R^\mu u \right)_{L^2(\Omega)} \right| + \left| \left({}_yD_D^\mu u,\ {}_yD_U^\mu u \right)_{L^2(\Omega)} \right| \right)^{\frac{1}{2}}, \tag{2.9}$$

and norm

$$\|u\|_{J_S^\mu(\Omega)} := \left(\|u\|_{L^2(\Omega)}^2 + |u|_{J_S^\mu(\Omega)}^2 \right)^{\frac{1}{2}}, \tag{2.10}$$

where $J_S^\mu(\Omega), J_{S,0}^\mu(\Omega)$ denote the closure of $C^\infty(\Omega), C_0^\infty(\Omega)$ with respect to $\|\cdot\|_{J_S^\mu(\Omega)}$.

LEMMA 2.1. *([10]) If $\mu > 0, \mu \neq n - \frac{1}{2}, n \in \mathbb{N}$, then $J^{\mu}_{L,0}(\Omega)$, $J^{\mu}_{R,0}(\Omega)$, $J^{\mu}_{S,0}(\Omega)$ and $H^{\mu}_{0}(\Omega)$ are equivalent with equivalent norms and semi-norms.*

LEMMA 2.2. *([10]) If $u \in J^{\mu}_{L,0}(\Omega)$, $0 < \eta < \mu$, then we have*

$$\|u\|_{L^2(\Omega)} \leq C_1 |u|_{J^{\mu}_{L}(\Omega)}, \quad |u|_{J^{\eta}_{L}(\Omega)} \leq C_1^{'} |u|_{J^{\mu}_{L}(\Omega)}. \tag{2.11}$$

If $u \in J^{\mu}_{R,0}(\Omega)$, $0 < \eta < \mu$, then we have

$$\|u\|_{L^2(\Omega)} \leq C_2 |u|_{J^{\mu}_{R}(\Omega)}, \quad |u|_{J^{\eta}_{R}(\Omega)} \leq C_2^{'} |u|_{J^{\mu}_{R}(\Omega)}, \tag{2.12}$$

where $C_1, C_1^{'}, C_2, C_2^{'}$ are some positive constants independent of u. Similar results can be followed for the fractional Sobolev space $H^{\mu}_{0}(\Omega)$ with $\mu \neq n - 1/2$, $n \in \mathbb{N}$.

LEMMA 2.3. *([10]) If $\mu > 0, \mu \neq n - \frac{1}{2}, n \in \mathbb{N}$, $u \in J^{\mu}_{L,0}(\Omega) \cap J^{\mu}_{R,0}(\Omega)$, then there exist positive constants C_1, C_1' and C_2, C_2' independent of u such that*

$$C_1 |u|_{H^{\mu}(\Omega)} \leq |u|_{J^{\mu}_{L}(\Omega)} \leq C_1' |u|_{H^{\mu}(\Omega)}, \tag{2.13}$$

$$C_2 |u|_{H^{\mu}(\Omega)} \leq |u|_{J^{\mu}_{R}(\Omega)} \leq C_2' |u|_{H^{\mu}(\Omega)}. \tag{2.14}$$

LEMMA 2.4. *([23]) For $u \in H^{\mu}_{0}(\Omega)$, $0 < \eta < \mu$, then there exist positive constants C_1, C_2, C_3, C_4 independent of u such that*

$$\|u\|_{L^2(\Omega)} \leq C_1 \|{}_{x}D^{\eta}_{L} u\|_{L^2(\Omega)} \leq C_2 \|{}_{x}D^{\mu}_{L} u\|_{L^2(\Omega)}, \tag{2.15}$$

$$\|u\|_{L^2(\Omega)} \leq C_3 \|{}_{y}D^{\eta}_{D} u\|_{L^2(\Omega)} \leq C_4 \|{}_{y}D^{\mu}_{D} u\|_{L^2(\Omega)}. \tag{2.16}$$

LEMMA 2.5. *([27]) If $\mu \in (1, 2), u, v \in J^{\mu}_{L,0}(\Omega)$ (or $J^{\mu}_{R,0}(\Omega)$), then*

$$({}_{x}D^{\mu}_{L} u, v)_{L^2(\Omega)} = ({}_{x}D^{\mu/2}_{L} u,\ {}_{x}D^{\mu/2}_{R} v)_{L^2(\Omega)},$$

$$({}_{y}D^{\mu}_{D} u, v)_{L^2(\Omega)} = ({}_{y}D^{\mu/2}_{D} u,\ {}_{y}D^{\mu/2}_{U} v)_{L^2(\Omega)},$$

$$({}_{x}D^{\mu}_{R} u, v)_{L^2(\Omega)} = ({}_{x}D^{\mu/2}_{R} u,\ {}_{x}D^{\mu/2}_{L} v)_{L^2(\Omega)},$$

$$({}_{y}D^{\mu}_{U} u, v)_{L^2(\Omega)} = ({}_{y}D^{\mu/2}_{U} u,\ {}_{y}D^{\mu/2}_{D} v)_{L^2(\Omega)}.$$

The proofs of the lemmas can be found in the corresponding references by considering u to be a zero-extension outside the domain Ω. Throughout the proceeding sections, we denote $(\cdot, \cdot) = (\cdot, \cdot)_{L^2(\Omega)}$, $\|\cdot\|_0 = \|\cdot\|_{L^2(\Omega)}$.

3. Crank-Nicolson Galerkin method for the two-dimensional time-space fractional wave equation

We first use the Crank-Nicolson finite difference scheme to approximate the Caputo time fractional derivative ${}_0^C D_t^\gamma u$ $(1<\gamma<2)$. Let $\tau = T/N$ be the time step, $t_n = n\tau, n = 0,1,...,N$. Denote $u(x,y,t_n) = u^n$, $u^{n-1/2} = \frac{u^n+u^{n-1}}{2}$, $\delta_t u^{n-1/2} = \frac{u^n-u^{n-1}}{\tau}$.

For $1<\gamma<2$, $n = 1,2,...N$, by [24], we have the Crank-Nicolson discrete scheme

$$\begin{aligned} {}_0^C D_t^\gamma u^{n-1/2} =& \frac{\tau^{1-\gamma}}{\Gamma(3-\gamma)}\Big[b_0^\gamma \delta_t u^{n-1/2} - \sum_{j=1}^{n-1}(b_{n-1-j}^\gamma - b_{n-j}^\gamma)\delta_t u^{j-1/2} - b_{n-1}^\gamma u_t^0\Big] \\ &+ R_n^\gamma, \end{aligned} \tag{3.1}$$

where $b_j^\gamma = (j+1)^{2-\gamma} - j^{2-\gamma}, j = 0,1,...,n-1$ satisfy $b_0^\gamma = 1$, $\sum_{j=1}^n b_{n-j}^\gamma = n^{2-\gamma}$, $\sum_{j=1}^{n-1}(b_{n-1-j}^\gamma - b_{n-j}^\gamma) + b_{n-1}^\gamma = 1$. The truncation error is given by

$$|R_n^\gamma| \le C \max_{0\le t\le T}\left|\frac{\partial^3 u(x,y,t)}{\partial t^3}\right| \tau^{3-\gamma}. \tag{3.2}$$

For $n \ge 1$, we denote

$$\overline{\nabla}_t^\gamma u^{n-1/2} = \frac{\tau^{1-\gamma}}{\Gamma(3-\gamma)}\Big[b_0^\gamma \delta_t u^{n-1/2} - \sum_{j=1}^{n-1}(b_{n-1-j}^\gamma - b_{n-j}^\gamma)\delta_t u^{j-1/2} - b_{n-1}^\gamma u_t^0\Big], \tag{3.3}$$

then we obtain the variational formulation of problem (1.1): find $u^n \in V$, such that

$$(\overline{\nabla} t^\gamma u^{n-1/2}, v) + B(u^{n-1/2}, v) = (f^{n-1/2}, v),\ \forall v \in V,\ t \in (0,T], \tag{3.4}$$

$$(u^0, v) = (\psi_0, v),\ \forall v \in V, \tag{3.5}$$

$$(u_t^0, v) = (\psi_1, v),\ \forall v \in V, \tag{3.6}$$

where $V = H_0^\alpha(\Omega) \cap H_0^\beta(\Omega)$. The bilinear form $B(u,v)$ is derived as

$$\begin{aligned} B(u,v) =& K_x c_\alpha \Big\{ ({}_xD_L^\alpha u,\ {}_xD_R^\alpha v) + ({}_xD_R^\alpha u,\ {}_xD_L^\alpha v)\Big\} \\ &+ K_y c_\beta \Big\{ ({}_yD_D^\beta u,\ {}_yD_U^\beta v) + ({}_yD_U^\beta u,\ {}_yD_D^\beta v)\Big\}. \end{aligned} \tag{3.7}$$

Assume that $\{\mathcal{T}_h\}$ is a family of unstructured triangulations of domain Ω and h is the maximum diameter of the triangular elements in $\mathcal{T}_h$. The conforming finite element space $V_h \in V$ is defined as

$$V_h = \{v_h | v_h \in C(\Omega) \cap V, v_h|_E \in P_s(E),\ \forall E \in \mathcal{T}_h\}, \tag{3.8}$$

where $P_s(E)$ is the set of polynomials with degree at most s in element E.

Let u_h^n be the finite element solution at time $t = t_n$, then the fully discrete Crank-Nicolson and Galerkin method (CNGM) for the time-space fractional wave equation can be expressed as: find $u_h^n \in V_h$ for $n = 1, 2, ..., N$ such that

$$(\overline{\nabla}_t^{\gamma} u_h^{n-1/2}, v_h) + B(u_h^{n-1/2}, v_h) = (f^{n-1/2}, v_h),\ \forall v_h \in V_h, \tag{3.9}$$

and

$$\begin{cases} u_h^0 = \mathcal{P}\psi_0(x, y), \\ (u_h^0)_t = \mathcal{P}\psi_1(x, y), \end{cases} \tag{3.10}$$

where $\mathcal{P} : L^2(\Omega) \to V_h$ is a projection operator.

Inserting Eq.(3.3) into Eq.(3.9), we obtain for $n > 1$,

$$\begin{aligned} 2\varpi(u_h^n, v_h) + \tau B(u_h^n, v_h) = & 2\varpi(u_h^{n-1}, v_h) + 2\tau\varpi b_{n-1}^{\gamma} \left((u_h^0)_t, v_h\right) \\ & + 2\varpi \sum_{j=1}^{n-1} (b_{n-1-j}^{\gamma} - b_{n-j}^{\gamma}) \left[(u_h^j, v_h) - (u_h^{j-1}, v_h)\right] \\ & - \tau B(u_h^{n-1}, v_h) + 2\tau \left(\frac{f^n + f^{n-1}}{2}, v_h\right),\ \forall v_h \in V_h, \end{aligned} \tag{3.11}$$

where $\varpi = \frac{\tau^{1-\gamma}}{\Gamma(3-\gamma)}$.

For $n = 1$, Eq.(3.9) yields

$$(\overline{\nabla}_t^{\gamma} u_h^{1/2}, v_h) + B(u_h^{1/2}, v_h) = (f^{1/2}, v_h),\ \forall v_h \in V_h, \tag{3.12}$$

that is

$$\begin{aligned} 2\varpi(u_h^1, v_h) + \tau B(u_h^1, v_h) = & 2\varpi(u_h^0, v_h) - \tau B(u_h^0, v_h) + 2\tau\varpi b_0^{\gamma} \left((u_h^0)_t, v_h\right) \\ & + 2\tau \left(\frac{f^1 + f^0}{2}, v_h\right),\ \forall v_h \in V_h. \end{aligned} \tag{3.13}$$

4. **Implementation of the unstructured mesh CNGM**

For the unstructured triangulations of a convex domain Ω, as shown in Fig. 4.1, the set of nodes are defined as $\{(x_k, y_k) : k = 1, 2, ..., N_p\}$, where N_p is the total number of nodes in the mesh. Let $\varphi_k(x_l, y_l) = \delta_{kl}, (k, l = 1, 2, ..., N_p)$ be the basis functions, where δ_{kl} is the Kronecker symbol. Then, for each time step $t = t_n$, the finite element solution u_h^n can be expressed as

$$u_h^n = \sum_{k=1}^{N_p} u_k^n \varphi_k(x, y). \tag{4.1}$$

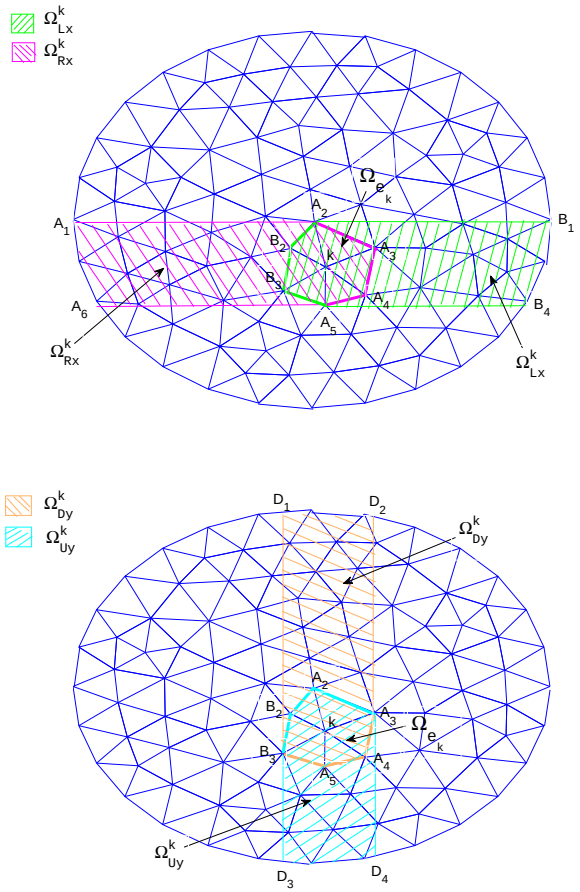

FIGURE 4.1. The unstructured triangular mesh of domain Ω with four nonzero support domains of the fractional derivative for node k. Ω^k_{Lx} is the nonzero support domain for ${}_xD^\alpha_L\varphi_k(x,y)$; Ω^k_{Rx} is for ${}_xD^\alpha_R\varphi_k(x,y)$, Ω^k_{Dy} is for ${}_yD^\beta_D\varphi_k(x,y)$, and Ω^k_{Uy} is for ${}_yD^\beta_U\varphi_k(x,y)$.

Choosing v_h be the basis function $\varphi_l(x,y)$, and inserting Eq.(4.1) into the finite element equations (3.11) and (3.13), then we have for $n=1$,

$$\sum_{k=1}^{N_p}(2\varpi(\varphi_k,\varphi_l)+\tau B(\varphi_k,\varphi_l))u_k^1 = 2\varpi(u_h^0,\varphi_l)-\tau B(u_h^0,\varphi_l) + 2\tau\varpi b_0^\gamma\left((u_h^0)_t,\varphi_l\right)+2\tau\left(\frac{f^1+f^0}{2},\varphi_l\right),\ l=1,2,...,N_p, \tag{4.2}$$

and for $n \geq 2$,

$$\sum_{k=1}^{N_p}(2\varpi(\varphi_k,\varphi_l)+\tau B(\varphi_k,\varphi_l))u_k^n = \sum_{k=1}^{N_p}(2\varpi(\varphi_k,\varphi_l)-\tau B(\varphi_k,\varphi_l))u_k^{n-1} + 2\varpi\sum_{j=1}^{n-1}(b_{n-1-j}^{\gamma}-b_{n-j}^{\gamma})\left[\sum_{k=1}^{N_p}(\varphi_k,\varphi_l)u_k^j-\sum_{k=1}^{N_p}(\varphi_k,\varphi_l)u_k^{j-1}\right] + 2\tau\varpi b_{n-1}^{\gamma}\left((u_h^0)_t,\varphi_l\right)+2\tau\left(\frac{f^n+f^{n-1}}{2},\varphi_l\right),\ l=1,2,...,N_p. \tag{4.3}$$

Eqs.(4.2) and (4.3) can be rewritten in matrix form as:

$$(2\varpi M+\tau A)\mathbf{u}^1 = 2\varpi W_1^0-\tau W_2^0+2\tau\varpi W_3^0+2\tau F^1,\ (n=1), \tag{4.4}$$

$$(2\varpi M+\tau A)\mathbf{u}^n = (2\varpi M-\tau A)\mathbf{u}^{n-1}+2\varpi M\sum_{j=1}^{n-1}(b_{n-1-j}^{\gamma}-b_{n-j}^{\gamma})(\mathbf{u}^j-\mathbf{u}^{j-1}) + 2\tau\varpi b_{n-1}^{\gamma}W_3^0+2\tau F^n,\ (n\geq 2), \tag{4.5}$$

where $\mathbf{u}^n=(u_1^n,u_2^n,...,u_{N_p}^n)^T$ is the unknown solution vector. The matrix $M=((\varphi_k,\varphi_l))_{N_p\times N_p}$ is the mass matrix, and $A=(B(\varphi_k,\varphi_l))_{N_p\times N_p}$ is the stiffness matrix. We also have the matrices $W_1^0=(w_1^1,w_1^2,...,w_1^{N_p})^T$, where $w_1^l=(u_h^0,\varphi_l)$; $W_2^0=(w_2^1,w_2^2,...,w_2^{N_p})^T$, where $w_2^l=B(u_h^0,\varphi_l)$; $W_3^0=(w_3^1,w_3^2,...,w_3^{N_p})^T$, where $w_3^l=\left((u_h^0)_t,\varphi_l\right)$; and $F^n=(F_1^n,F_2^n,...,F_{N_p}^n)^T$, $F_l^n=\left(\frac{f^n+f^{n-1}}{2},\varphi_l\right)$, $l=1,2,...,N_p$, $n=1,2,...,N$.

In order to calculate the inner product elements in the matrices, for example (φ_k,φ_l), the following Gauss quadrature formula [7, 8] will be used:

$$\begin{aligned}(\varphi_k,\varphi_l) &= \int_\Omega \varphi_k\cdot\varphi_l dxdy\\ &= \sum_{E\in\mathcal{T}_h}\int_E \varphi_k\cdot\varphi_l dxdy\\ &= \sum_{E\in\mathcal{T}_h}\sum_{(x_{ci},y_{ci})\in G_E}\varphi_k|_{(x_{ci},y_{ci})}\cdot\varphi_l|_{(x_{ci},y_{ci})}\cdot\omega_i,\end{aligned} \tag{4.6}$$

where G_E is the set of the Gauss points in a certain element E and ω_i are the weights corresponding to the Gauss points (x_{ci},y_{ci}).

As a result of the non-local characteristics of the fractional derivatives, compared with the finite element method used for solving traditional differential equations, the implementation of the finite element scheme for fractional differential equations is much more complex. In order to obtain the unknown solution vector $\mathbf{u}^n$ given in Eqs. (4.4) and (4.5), constructing the matrix A will be the most critical part. The (k,l) element in the matrix A is given by

$$\begin{aligned} B(\varphi_k,\varphi_l) =& K_x c_\alpha \Big\{ ({}_xD_L^\alpha\varphi_k,\ {}_xD_R^\alpha\varphi_l) + ({}_xD_R^\alpha\varphi_k,\ {}_xD_L^\alpha\varphi_l) \Big\} \\ &+ K_y c_\beta \Big\{ ({}_yD_D^\beta\varphi_k,\ {}_yD_U^\beta\varphi_l) + ({}_yD_U^\beta\varphi_k,\ {}_yD_D^\beta\varphi_l) \Big\}. \end{aligned} \tag{4.7}$$

There are four components to approximate in the right hand of Eq.(4.7). Taking the first component $({}_xD_L^\alpha\varphi_k,\ {}_xD_R^\alpha\varphi_l)$ as an example, application of Gauss quadrature yields:

$$\begin{aligned} ({}_xD_L^\alpha\varphi_k,\ {}_xD_R^\alpha\varphi_l) &= \int_\Omega {}_xD_L^\alpha\varphi_k \cdot\ {}_xD_R^\alpha\varphi_l dxdy \\ &= \sum_{E\in\mathcal{T}_h} \int_E {}_xD_L^\alpha\varphi_k \cdot\ {}_xD_R^\alpha\varphi_l dxdy \\ &= \sum_{E\in\mathcal{T}_h} \sum_{(x_{ci},y_{ci})\in G_E} {}_xD_L^\alpha\varphi_k|_{(x_{ci},y_{ci})} \cdot\ {}_xD_R^\alpha\varphi_l|_{(x_{ci},y_{ci})} \cdot \omega_i. \end{aligned} \tag{4.8}$$

To calculate the non-local fractional derivatives ${}_xD_L^\alpha\varphi_k(x,y)|_{(x_{ci},y_{ci})}$ $({}_xD_L^\alpha\varphi_l(x,y)|_{(x_{ci},y_{ci})})$, the piecewise continuous basis functions $\varphi_k(x,y)$ $(\varphi_l(x,y))$ should be formed first.

As is well known, for a certain triangle $\triangle(1,2,3)$, the nodes $(1,2,3)$ with coordinates $(x_i,y_i)(i=1,2,3)$ are numbered in a counter-clockwise order. The corresponding values of the function $u(x,y)$ are labelled as u_1,u_2,u_3. The element basis functions for $\triangle(1,2,3)$ can be written as

$$N_i(x,y) = \frac{1}{2A_*}(a_i + b_i x + c_i y), i = 1,2,3, \tag{4.9}$$

where A_* is the area of the triangle expressed by the absolute value of $\widetilde{A}$, where $\widetilde{A} = \frac{1}{2}\begin{vmatrix} 1 & x_1 & y_1 \\ 1 & x_2 & y_2 \\ 1 & x_3 & y_3 \end{vmatrix}$, $a_i = x_j y_k - x_k y_j, b_i = y_j - y_k, c_i = x_k - x_j$, the subscripts $(i,j,k) = (1,2,3)$ or $(2,3,1)$ or $(3,1,2)$. Then the function $u(x,y)$ on triangle $\triangle(1,2,3)$ can be approximated by

$$u(x,y) = \sum_{i=1}^{3} N_i(x,y)u_i. \tag{4.10}$$

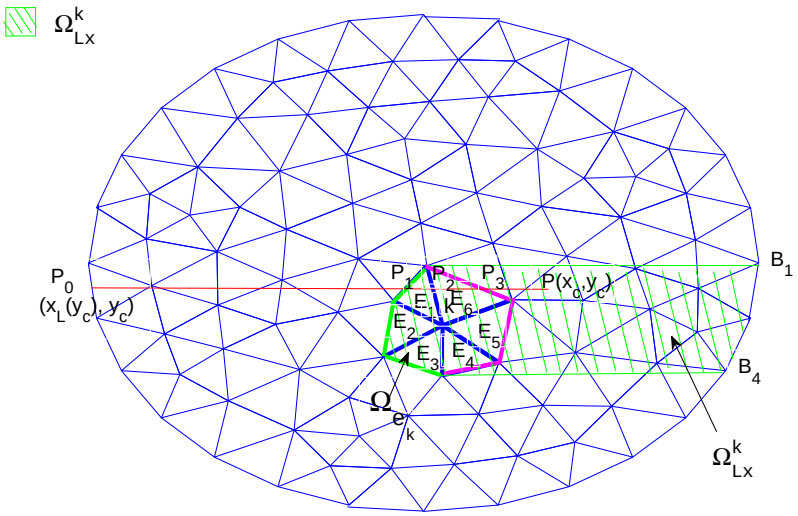

FIGURE 4.2. The support domain Ω_{e_k} composed of six triangular elements $E_1, E_2, ..., E_6$, and the nonzero support domain Ω^k_{Lx} for the fractional derivative operator ${}_xD^\alpha_L\varphi_k(x,y)$.

On this basis, according to the unstructured triangular mesh shown in Fig. 4.1, every node k is a common vertex of the neighboring triangular elements. The support domain of the basis function $\varphi_k(x,y)$ is a polygon composed by triangles sharing the common node k, denoted by Ω_{e_k}, enclosed with sides $\overline{A_2A_3}, \overline{A_3A_4}, \overline{A_4A_5}, \overline{A_5B_3}, \overline{B_3B_2}$.

As shown in Fig. 4.2, noting that the support domain Ω_{e_k} is composed of six triangular elements $E_1, E_2, ..., E_6$, then by combining the local element basis function $N_k(x,y)$ of each triangle, we can form the piecewise continuous basis function $\varphi_k(x,y)$. Since $\forall(x,y) \in \partial\Omega_{e_k}$, $\varphi_k(x,y) = 0$, the domain of definition of the basis function $\varphi_k(x,y)$ can be extended from Ω_{e_k} to the whole domain Ω.

It follows that only when the Gauss point $P(x_c, y_c)$ is within the region Ω^k_{Lx}, (shown in Fig. 4.2), the corresponding value of ${}_xD^\alpha_L\varphi_k(x_c, y_c)$ is nonzero. Thus, $\forall P(x_c, y_c) \in \Omega^k_{Lx}$, by the definition given in Eq. (1.5), we

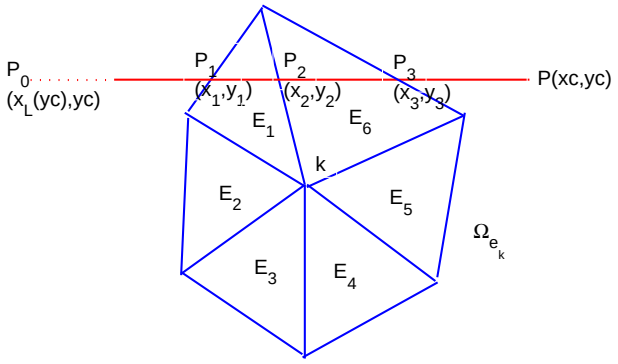

FIGURE 4.3. The support domain Ω_{e_k} intersected by the line $y = y_c$.

have

$$
\begin{aligned}
{}_xD_L^{\alpha}\varphi_k(x_c,y_c) &= \left({}_{x_L(y_c)}D_x^{\alpha}\varphi_k(x,y_c)\right)|_{x=x_c} \\
&= \left(\frac{1}{\Gamma(1-\alpha)}\frac{d}{dx}\int_{x_L(y_c)}^{x}(x-s)^{-\alpha}\varphi_k(s,y_c)ds \right)_{x=x_c},
\end{aligned} \tag{4.11}
$$

which requires an integeral from the left boundary $x_L(y_c)$ to x_c. As is shown is Fig. 4.3, the line $y = y_c$ intersects the support domain Ω_{e_k} at three points $P_1(x_1, y_1), P_2(x_2, y_2)$, and $P_3(x_3, y_3)$. The basis function $\varphi_k(x, y_c)$ can be written in the following interpolation form:

$$
\varphi_k(x,y_c) = \begin{cases} 0, \ x < x_1 \ \texttt{or} \ x > x_3, \\ \varphi_{k1}(x,y_c) = \frac{x-x_2}{x_1-x_2}z_1 + \frac{x-x_1}{x_2-x_1}z_2, \ x_1 \le x < x_2, \\ \varphi_{k2}(x,y_c) = \frac{x-x_3}{x_2-x_3}z_2 + \frac{x-x_2}{x_3-x_2}z_3, \ x_2 \le x \le x_3, \end{cases} \tag{4.12}
$$

where $z_i = \varphi_k(x_i, y_c), (i = 1, 2, 3)$ are the values of $\varphi_k(x, y)$ at points P_1, P_2, P_3, which can be obtained by two-point interpolation between the

two vertices of the triangle edge. We have that

$$ {}_xD_L^\alpha\varphi_k(x,y_c)=\begin{cases} 0, x<x_1, \\ {}_{x_1}D_x^\alpha\varphi_{k1}(x,y_c), x_1\le x<x_2, \\ {}_{x_1}D_{x_2}^\alpha\varphi_{k1}(x,y_c)+\ {}_{x_2}D_x^\alpha\varphi_{k2}(x,y_c), x_2\le x<x_3, \\ {}_{x_1}D_{x_2}^\alpha\varphi_{k1}(x,y_c)+\ {}_{x_2}D_{x_3}^\alpha\varphi_{k2}(x,y_c), x_3\le x. \end{cases} \tag{4.13} $$

Inserting Eq.(4.12) into Eq.(4.13), and noting that on $\partial\Omega_{e_k}$, $z_1=z_3=0$, we have

$$ {}_xD_L^\alpha\varphi_k(x,y_c)=\begin{cases} 0,\ x<x_1, \\ \omega\lambda_1(x-x_1)^{1-\alpha},\ x_1\le x<x_2, \\ \omega\lambda_1(x-x_1)^{1-\alpha}+\omega(\lambda_2-\lambda_1)(x-x_2)^{1-\alpha},\ x_2\le x<x_3, \\ \omega\lambda_1(x-x_1)^{1-\alpha}+\omega(\lambda_2-\lambda_1)(x-x_2)^{1-\alpha} \\ \qquad\qquad -\omega\lambda_2(x-x_3)^{1-\alpha},\ x_3\le x, \end{cases} \tag{4.14} $$

where $\omega=\frac{1}{\Gamma(2-\alpha)}, \lambda_i=\frac{z_{i+1}-z_i}{x_{i+1}-x_i}, (i=1,2,3)$. We then find the interval to which x_c belongs, and replace x with x_c to obtain ${}_xD_L^\alpha\varphi_k(x_c,y_c)$.

Similarly, the fractional derivatives ${}_xD_R^\alpha\varphi_k(x_c,y_c)$, ${}_yD_D^\beta\varphi_k(x_c,y_c)$ and ${}_yD_U^\beta\varphi_k(x_c,y_c)$ can also be calculated with support domains being Ω_{Rx}^k, Ω_{Dy}^k, Ω_{Uy}^k (shown in Fig. 4.1), respectively. This procedure allows the matrix A to be formed.

For each node k $(k=1,2,...,N_p)$, Algorithm 1 summarizes the algorithm for calculating ${}_xD_L^\alpha\varphi_k(x_c,y_c)$.

5. **Stability and convergence**

To analyse the stability and convergence of the fully discrete scheme CNGM, some definitions and lemmas should be given in advance. Based on the bilinear form $B(u,v)$, the semi-norm $|\cdot|_{(\alpha,\beta)}$ and the norm $\|\cdot\|_{(\alpha,\beta)}$ are defined as:

$$ |u|_{(\alpha,\beta)}=\left(K_x\|{}_xD_L^\alpha u\|_0^2+K_y\|{}_yD_D^\beta u\|_0^2\right)^{1/2}, \tag{5.1} $$

$$ \|u\|_{(\alpha,\beta)}=\left(\|u\|_0^2+|u|_{(\alpha,\beta)}^2\right)^{1/2}. \tag{5.2} $$

Throughout the following sections, we suppose C is a positive constant that may be different depending on the context.

5.1. **Stability.**

Algorithm 1 The algorithm for the calculation of ${}_xD_L^\alpha\varphi_k(x_c,y_c)$.

Partition the convex domain Ω using an unstructured triangular mesh via a suitable mesh generation software; Output the numbered nodes and corresponding coordinates (x_k,y_k) $(k=1,2,...,N_p)$, and the triangular elements $E_j\in\mathcal{T}_h$ $(j=1,2,...,N_e)$ characterized by three vertices.

for $k=1,2,...,N_p$ **do**
  for $j=1,2,...,N_e$ **do**
    if the vertices of the element E_j include the node k **then**
      $E_j\in\Omega_{e_k}$
    end if
    Generate the set of Gauss points $G_{E_j}=\{(x_{ci},y_{ci})|i=1,...,N_g^2\}$ for each element E_j and the corresponding weights ω_i. Here N_g is a control parameter and is usually chosen as 1 or 2.
  end for
  Construct the support domain Ω_{e_k} of the basis function $\varphi_k(x,y)$.
  Calculate the $\underline{y_k}=\min\{y|(x,y)\in\Omega_{e_k}\}$, $\overline{y_k}=\max\{y|(x,y)\in\Omega_{e_k}\}$, then construct the nonzero support domain Ω_{Lx}^k of the fractional derivative ${}_xD_L^\alpha\varphi_k(x,y)$, which is enclosed by the left-side boundary of Ω_{e_k}, the right boundary $x_R(y)$ of domain Ω, line $y=\underline{y_k}$ and line $y=\overline{y_k}$, as shown in Fig. 4.2.
  for all Gauss point $(x_c,y_c)\in G_{E_1}\cup G_{E_2}\cdots\cup G_{E_{N_e}}$ **do**
    if $(x_c,y_c)\in\Omega_{Lx}^k$ **then**
      Intersect Ω_{e_k} with line $y=y_c$, calculate the coordinates of the intersection points and corresponding values of z_i on each intersection point, as shown in Fig. 4.3.
      Form the piecewise continuous basis function $\varphi_k(x,y_c)$ given by Eq.(4.12), and then calculate the ${}_xD_L^\alpha\varphi_k(x_c,y_c)$ based on Eqs. (4.13)-(4.14).
    else
      ${}_xD_L^\alpha\varphi_k(x_c,y_c)=0$
    end if
  end for
end for

LEMMA 5.1. *For $u\in V$, the semi-norm $|\cdot|_{(\alpha,\beta)}$ and norm $\|\cdot\|_{(\alpha,\beta)}$ are equivalent, and the following inequality holds*

$$C_1\|u\|_{(\alpha,\beta)}\le|u|_{(\alpha,\beta)}\le\|u\|_{(\alpha,\beta)}\le C_2|u|_{H^\mu(\Omega)},\tag{5.3}$$

where C_1,C_2 are positive constants independent of u.

P r o o f. By definitions (5.1)-(5.2), we have that

$$|u|_{(\alpha,\beta)} \leq \|u\|_{(\alpha,\beta)}. \tag{5.4}$$

By lemma 2.4, there exists a constant C, such that $\|u\|_0 \leq C|u|_{(\alpha,\beta)}$. Then

$$\|u\|_{(\alpha,\beta)} \leq \left(C|u|^2_{(\alpha,\beta)} + |u|^2_{(\alpha,\beta)}\right)^{1/2} \leq C'|u|_{(\alpha,\beta)}. \tag{5.5}$$

Thus,

$$C_1\|u\|_{(\alpha,\beta)} \leq |u|_{(\alpha,\beta)}, \text{ where } C_1 = \frac{1}{\sqrt{C'^2+1}}. \tag{5.6}$$

By lemma 2.4 again, $|u|_{(\alpha,\beta)} \leq C|u|_{J_L^\lambda(\Omega)}$ and lemma 2.3 gives

$$\|u\|_{(\alpha,\beta)} \leq \frac{1}{C_1}|u|_{(\alpha,\beta)} \leq \frac{C}{C_1}|u|_{J_L^\lambda(\Omega)} \leq C_2|u|_{H^\mu(\Omega)} \tag{5.7}$$

Then the proof can be completed by combining (5.4), (5.6) and (5.7). □

Lemma 5.2. *([3]) The bilinear form $B(u,v)$ is symmetrical, continuous and coercive, and therefore $\exists\, C_1, C_2$ satisfying*

$$B(u,v) \leq C_1\|u\|_{(\alpha,\beta)}\|v\|_{(\alpha,\beta)}, B(u,u) \geq C_2\|u\|^2_{(\alpha,\beta)},\ \forall u,v \in H_0^\alpha(\Omega)\cap H_0^\beta(\Omega). \tag{5.8}$$

Theorem 5.1. *(Stability) The fully discrete CNGM scheme (3.9) is unconditionally stable.*

P r o o f. Suppose that $\widetilde{u}_h^n$ is an approximate numerical solution of (3.9), let $\varepsilon_h^n = u_h^n - \widetilde{u}_h^n$, then $\varepsilon_h^{n-1/2}$ satisfies

$$(\overline{\nabla}_t^\gamma \varepsilon_h^{n-1/2}, v_h) + B(\varepsilon_h^{n-1/2}, v_h) = 0,\ \forall v_h \in V_h. \tag{5.9}$$

Let $v_h = \delta_t \varepsilon_h^{n-1/2}$ in (5.9), then we have

$$\begin{aligned}\varpi b_0^\gamma \|\delta_t\varepsilon_h^{n-1/2}\|_0^2 + B(\varepsilon_h^{n-1/2}, \delta_t\varepsilon_h^{n-1/2}) &= \varpi b_{n-1}^\gamma \left((\varepsilon_h^0)_t, \delta_t\varepsilon_h^{n-1/2}\right) \\ &+ \varpi \sum_{j=1}^{n-1}(b_{n-1-j}^\gamma - b_{n-j}^\gamma)\left(\delta_t\varepsilon_h^{j-1/2}, \delta_t\varepsilon_h^{n-1/2}\right).\end{aligned} \tag{5.10}$$

Using the Cauchy-Schwarz inequality,

$$\begin{aligned}\varpi\|\delta_t\varepsilon_h^{n-1/2}\|_0^2 + B(\varepsilon_h^{n-1/2}, \delta_t\varepsilon_h^{n-1/2}) &\leq \frac{\varpi}{2} b_{n-1}^\gamma \left(\|(\varepsilon_h^0)_t\|_0^2 + \|\delta_t\varepsilon_h^{n-1/2}\|_0^2\right) \\ &+ \frac{\varpi}{2}\sum_{j=1}^{n-1}(b_{n-1-j}^\gamma - b_{n-j}^\gamma)\cdot\left(\|\delta_t\varepsilon_h^{j-1/2}\|_0^2 + \|\delta_t\varepsilon_h^{n-1/2}\|_0^2\right).\end{aligned} \tag{5.11}$$

Noting that $\sum_{j=1}^{n-1}(b_{n-1-j}^{\gamma}-b_{n-j}^{\gamma})+b_{n-1}^{\gamma}=1$, $\varepsilon_h^{n-1/2}=\frac{\varepsilon_h^n+\varepsilon_h^{n-1}}{2}$ and $\delta_t\varepsilon_h^{n-1/2}=\frac{\varepsilon_h^n-\varepsilon_h^{n-1}}{\tau}$, Eq.(5.11) can be rewritten as

$$\begin{aligned}\frac{\varpi}{2}\|\delta_t\varepsilon_h^{n-1/2}\|_0^2+\frac{1}{2\tau}\left(B(\varepsilon_h^n,\varepsilon_h^n)-B(\varepsilon_h^{n-1},\varepsilon_h^{n-1})\right)\le\frac{\varpi}{2}b_{n-1}^{\gamma}\|(\varepsilon_h^0)_t\|_0^2\\+\frac{\varpi}{2}\sum_{j=1}^{n-1}(b_{n-1-j}^{\gamma}-b_{n-j}^{\gamma})\|\delta_t\varepsilon_h^{j-1/2}\|_0^2.\end{aligned}\tag{5.12}$$

Then we have

$$\begin{aligned}\tau\varpi\|\delta_t\varepsilon_h^{n-1/2}\|_0^2+B(\varepsilon_h^n,\varepsilon_h^n)+\tau\varpi\sum_{j=1}^{n-1}b_{n-j}^{\gamma}\|\delta_t\varepsilon_h^{j-1/2}\|_0^2\le B(\varepsilon_h^{n-1},\varepsilon_h^{n-1})\\+\tau\varpi\sum_{j=1}^{n-1}b_{n-1-j}^{\gamma}\|\delta_t\varepsilon_h^{j-1/2}\|_0^2+\tau\varpi b_{n-1}^{\gamma}\|(\varepsilon_h^0)_t\|_0^2.\end{aligned}\tag{5.13}$$

Denote

$$l^n=B(\varepsilon_h^n,\varepsilon_h^n)+\tau\varpi\sum_{j=1}^{n}b_{n-j}^{\gamma}\|\delta_t\varepsilon_h^{j-1/2}\|_0^2,\tag{5.14}$$

then from (5.13) we obtain

$$\begin{aligned}l^n&\le l^{n-1}+\tau\varpi b_{n-1}^{\gamma}\|(\varepsilon_h^0)_t\|_0^2\\&\le l^{n-2}+\tau\varpi b_{n-2}^{\gamma}\|(\varepsilon_h^0)_t\|_0^2+\tau\varpi b_{n-1}^{\gamma}\|(\varepsilon_h^0)_t\|_0^2\\&\cdots\\&\le l^0+\tau\varpi\sum_{j=1}^{n}b_{n-j}^{\gamma}\|(\varepsilon_h^0)_t\|_0^2.\end{aligned}\tag{5.15}$$

Since $\sum_{j=1}^{n}b_{n-j}^{\gamma}=n^{2-\gamma}$, $\tau\varpi=\frac{\tau^{2-\gamma}}{\Gamma(3-\gamma)}$, $\tau n\le T$, we have

$$l^n\le l^0+\frac{T^{2-\gamma}}{\Gamma(3-\gamma)}\|(\varepsilon_h^0)_t\|_0^2.\tag{5.16}$$

Returning to (5.14), note that

$$\tau\varpi\sum_{j=1}^{n-1}b_{n-j}^{\gamma}\|\delta_t\varepsilon_h^{j-1/2}\|_0^2\ge 0,\tag{5.17}$$

and therefore

$$B(\varepsilon_h^n,\varepsilon_h^n)\le B(\varepsilon_h^0,\varepsilon_h^0)+\frac{T^{2-\gamma}}{\Gamma(3-\gamma)}\|(\varepsilon_h^0)_t\|_0^2.\tag{5.18}$$

By lemma 5.2, it can be obtained that

$$\|\varepsilon_h^n\|_{(\alpha,\beta)}^2 \le C\left(\|\varepsilon_h^0\|_{(\alpha,\beta)}^2 + \|(\varepsilon_h^0)_t\|_0^2\right). \tag{5.19}$$

Hence, the fully discrete CNGM scheme is unconditionally stable. □

5.2. **Convergence.** To proceed with the convergence analysis for the fully discrete scheme CNGM shown in (3.9), we suppose that for $u \in H^\mu(\Omega)$, $0 < \mu \le s+1$, $0 \le \nu \le \mu$, there exists a constant C such that

$$\|u - \Pi_h u\|_{H^\nu(\Omega)} \le Ch^{\mu-\nu}\|u\|_{H^\mu(\Omega)}, \tag{5.20}$$

where $\Pi_h : H^{s+1}(\Omega) \to V_h$ is an interpolation operator [9]. For $u \in V$, we define a projection operator $P_h : V \to V_h$ characterized by

$$B(u, v_h) = B(P_h u, v_h),\ \forall v_h \in V_h. \tag{5.21}$$

An approximation property of the operator P_h can be obtained via the following lemma.

LEMMA 5.3. *([4]) If $u \in H^\mu(\Omega) \cap V$, $\lambda < \mu \le s+1$, $\lambda = \max\{\alpha, \beta\}$, then there exists a constant C independent of h and u such that*

$$|u - P_h u|_{(\alpha,\beta)} \le Ch^{\mu-\lambda}\|u\|_{H^\mu(\Omega)}. \tag{5.22}$$

THEOREM 5.2. *(Convergence) Assume that $u^n = u(x, y, t_n)$ is the exact solution of problem (1.1) with $u, u_{ttt}, {}_0^C D_t^\gamma u \in L^\infty(H^\mu(\Omega); 0, T)$, $\lambda < \mu \le s+1$, $\lambda = \max\{\alpha, \beta\}$, then the numerical solution u_h^n satisfies*

$$\begin{aligned}\|u_h^n - u^n\|_{(\alpha,\beta)}^2 \le{}& Ch^{2\mu-2\lambda}\left(\|u^n\|_{H^\mu(\Omega)}^2 + \|u^0\|_{H^\mu(\Omega)}^2 + \|u_t^0\|_{H^\mu(\Omega)}^2\right)\\ &+ C\left\{\tau^{2(3-\gamma)} + h^{2\mu-2\lambda}\max_{1\le j\le n}\|\,{}_0^C D_t^\gamma u^{j-1/2}\|_{H^\mu(\Omega)}^2\right\}.\end{aligned} \tag{5.23}$$

P r o o f. $\forall v_h \in V_h$ we have

$$({}_0^C D_t^\gamma u^{n-1/2}, v_h) + B(u^{n-1/2}, v_h) = (f^{n-1/2}, v_h), \tag{5.24}$$

$$(\overline{\nabla}_t^\gamma u_h^{n-1/2}, v_h) + B(u_h^{n-1/2}, v_h) = (f^{n-1/2}, v_h). \tag{5.25}$$

Let $e^n = u_h^n - u^n$, then $e^{n-1/2}$ satisfies

$$(\overline{\nabla}_t^\gamma e^{n-1/2}, v_h) + B(e^{n-1/2}, v_h) = ({}_0^C D_t^\gamma u^{n-1/2} - \overline{\nabla}_t^\gamma u^{n-1/2}, v_h). \tag{5.26}$$

Denote $e^{n-1/2} = \theta^{n-1/2} + \rho^{n-1/2}$, where $\rho^{n-1/2} = P_h u^{n-1/2} - u^{n-1/2}$, $\theta^{n-1/2} = u_h^{n-1/2} - P_h u^{n-1/2}$. Noting that $B(\rho^{n-1/2}, v_h) = 0$, and taking

$v_h = \delta_t\theta^{n-1/2}$, then equation (5.26) can be rewritten as

$$(\overline{\nabla}_t^{\gamma}\theta^{n-1/2},\delta_t\theta^{n-1/2}) + B(\theta^{n-1/2},\delta_t\theta^{n-1/2}) = ({}_0^C D_t^{\gamma}u^{n-1/2} - \overline{\nabla}_t^{\gamma}u^{n-1/2},\delta_t\theta^{n-1/2}) - (\overline{\nabla}_t^{\gamma}\rho^{n-1/2},\delta_t\theta^{n-1/2}). \tag{5.27}$$

Let $\overline{R}_n = {}_0^C D_t^{\gamma}u^{n-1/2} - \overline{\nabla}_t^{\gamma}u^{n-1/2} - \overline{\nabla}_t^{\gamma}\rho^{n-1/2}$,

$$\varpi\Big(\Big[b_0^{\gamma}\delta_t\theta^{n-1/2} - \sum_{j=1}^{n-1}(b_{n-1-j}^{\gamma}-b_{n-j}^{\gamma})\delta_t\theta^{j-1/2} - b_{n-1}^{\gamma}\theta_t^0\Big],\delta_t\theta^{n-1/2}\Big) + B(\theta^{n-1/2},\delta_t\theta^{n-1/2}) = (\overline{R}_n,\delta_t\theta^{n-1/2}). \tag{5.28}$$

Since $B(\theta^{n-1/2},\delta_t\theta^{n-1/2}) = \frac{1}{2\tau}\big(B(\theta^n,\theta^n) - B(\theta^{n-1},\theta^{n-1})\big)$, then by the Cauchy-Schwarz inequality, we have

$$\begin{aligned} 2\tau\varpi\|\delta_t\theta^{n-1/2}\|_0^2 + B(\theta^n,\theta^n) &\le B(\theta^{n-1},\theta^{n-1})) \\ &+ 2\tau\varpi\sum_{j=1}^{n-1}(b_{n-1-j}^{\gamma} - b_{n-j}^{\gamma})\|\delta_t\theta^{k-1/2}\|_0\ \|\delta_t\theta^{n-1/2}\|_0 \\ &+ 2\tau\varpi b_{n-1}^{\gamma}\|\theta_t^0\|_0\ \|\delta_t\theta^{n-1/2}\|_0 + 2\tau(\overline{R}_n,\delta_t\theta^{n-1/2}) \end{aligned} \tag{5.29}$$

Similar to the proof of stability, by using the Cauchy- Schwarz inequality, the inequality (5.29) can be rewritten as

$$\begin{aligned} \tau\varpi\|\delta_t\theta^{n-1/2}\|_0^2 + B(\theta^n,\theta^n) + \tau\varpi\sum_{j=1}^{n-1} b_{n-j}^{\gamma}\|\delta_t\theta^{k-1/2}\|_0^2 &\le B(\theta^{n-1},\theta^{n-1}) + \tau\varpi\sum_{j=1}^{n-1} b_{n-1-j}^{\gamma}\|\delta_t\theta^{k-1/2}\|_0^2 \\ &+ \tau\varpi b_{n-1}^{\gamma}\|\theta_t^0\|_0^2 + 2\tau(\overline{R}_n,\delta_t\theta^{n-1/2}). \end{aligned} \tag{5.30}$$

Let

$$E^n = B(\theta^n,\theta^n) + \tau\varpi\sum_{j=1}^{n} b_{n-j}^{\gamma}\|\delta_t\theta^{j-1/2}\|_0^2, \tag{5.31}$$

then we have

$$\begin{aligned} E^n \leq & E^{n-1} + \tau\varpi b_{n-1}^{\gamma}\|\theta_t^0\|_0^2 + 2\tau(\overline{R}_n, \delta_t\theta^{n-1/2}) \\ & \leq E^0 + \tau\varpi\sum_{j=1}^{n} b_{n-j}^{\gamma}\|\theta_t^0\|_0^2 + \sum_{j=1}^{n} 2\tau(\overline{R}_j, \delta_t\theta^{j-1/2}) \\ & \leq E^0 + \frac{T^{2-\gamma}}{\Gamma(3-\gamma)}\|\theta_t^0\|_0^2 + \sum_{j=1}^{n} 2\tau(\overline{R}_j, \delta_t\theta^{j-1/2}). \end{aligned} \tag{5.32}$$

That is

$$\begin{aligned} B(\theta^n, \theta^n) + \tau\varpi\sum_{j=1}^{n} b_{n-j}^{\gamma}\|\delta_t\theta^{j-1/2}\|_0^2 \leq B(\theta^0, \theta^0) + \frac{T^{2-\gamma}}{\Gamma(3-\gamma)}\|\theta_t^0\|_0^2 \\ + \sum_{j=1}^{n} 2\tau(\overline{R}_j, \delta_t\theta^{j-1/2}). \end{aligned} \tag{5.33}$$

Since

$$\begin{aligned} \sum_{j=1}^{n} 2\tau(\overline{R}_j, \delta_t\theta^{j-1/2}) &= 2\tau\sum_{j=1}^{n}\Big(\frac{1}{\sqrt{\varpi b_{n-j}^{\gamma}}}\overline{R}_j, \sqrt{\varpi b_{n-j}^{\gamma}}\delta_t\theta^{j-1/2}\Big) \\ &\leq 2\tau\sum_{j=1}^{n}\Big(\frac{1}{2\varpi b_{n-j}^{\gamma}}\|\overline{R}_j\|_0^2 + \frac{\varpi b_{n-j}^{\gamma}}{2}\|\delta_t\theta^{j-1/2}\|_0^2\Big) \\ &= \frac{\tau}{\varpi}\sum_{j=1}^{n}\frac{1}{b_{n-j}^{\gamma}}\|\overline{R}_j\|_0^2 + \tau\varpi\sum_{j=1}^{n} b_{n-j}^{\gamma}\|\delta_t\theta^{j-1/2}\|_0^2, \end{aligned} \tag{5.34}$$

then we have

$$B(\theta^n, \theta^n) \leq B(\theta^0, \theta^0) + \frac{T^{2-\gamma}}{\Gamma(3-\gamma)}\|\theta_t^0\|_0^2 + C\max_{1\leq j\leq n}\|\overline{R}_j\|_0^2. \tag{5.35}$$

By lemma 5.2, the inequality (5.35) yields

$$\|\theta^n\|_{(\alpha,\beta)}^2 \leq C\|\theta^0\|_{(\alpha,\beta)}^2 + C\frac{T^{2-\gamma}}{\Gamma(3-\gamma)}\|\theta_t^0\|_0^2 + C\max_{1\leq j\leq n}\|\overline{R}_j\|_0^2. \tag{5.36}$$

By the Minkowski inequality and lemma 5.3,

$$\begin{aligned} \|\theta^0\|_{(\alpha,\beta)}^2 = \|u_h^0 - P_h u^0\|_{(\alpha,\beta)}^2 &= \|u_h^0 - u^0 + u^0 - P_h u^0\|_{(\alpha,\beta)}^2 \\ &\leq C\Big(\|u_h^0 - u^0\|_{(\alpha,\beta)}^2 + \|u^0 - P_h u^0\|_{(\alpha,\beta)}^2\Big) \\ &\leq C\|u_h^0 - u^0\|_{(\alpha,\beta)}^2 + Ch^{2\mu-2\lambda}\|u^0\|_{H^{\mu}(\Omega)}^2. \end{aligned} \tag{5.37}$$

Note that $\|\cdot\|_0 \le C\|\cdot\|_{(\alpha,\beta)}$, then

$$\begin{aligned}\|\theta_t^0\|_0 = \|(u_h^0 - P_h u^0)_t\|_0^2 &= \|(u_h^0 - u^0 + u^0 - P_h u^0)_t\|_0^2 \\ &\le C\Big(\|(u_h^0)_t - u_t^0\|_0^2 + \|u_t^0 - P_h u_t^0)\|_0^2\Big) \\ &\le C\|(u_h^0)_t - u_t^0\|_0^2 + Ch^{2\mu-2\lambda}\|u_t^0\|_{H^\mu(\Omega)}^2.\end{aligned} \tag{5.38}$$

The term $\|\overline{R}_j\|_0^2$ can be estimated as

$$\begin{aligned}\|\overline{R}_j\|_0^2 =& \|\ {}_0^C D_t^\gamma u^{j-1/2} - \overline{\nabla}_t^\gamma u^{j-1/2} - \overline{\nabla}_t^\gamma \rho^{j-1/2}\|_0^2 \\ &\le C\Big(\|\ {}_0^C D_t^\gamma u^{j-1/2} - \overline{\nabla}_t^\gamma u^{j-1/2}\|_0^2 + \|\overline{\nabla}_t^\gamma \rho^{j-1/2}\|_0^2\Big) \\ &\le C\tau^{2(3-\gamma)} \max_{0\le t\le T}\|u_{ttt}\|_0^2 + C\|\overline{\nabla}_t^\gamma \rho^{j-1/2}\|_0^2 \\ &\le C\tau^{2(3-\gamma)} + C\|\overline{\nabla}_t^\gamma \rho^{j-1/2}\|_0^2.\end{aligned} \tag{5.39}$$

By lemma 5.3,

$$\begin{aligned}\|\overline{\nabla}_t^\gamma \rho^{j-1/2}\|_0^2 =& \|\overline{\nabla}_t^\gamma \rho^{j-1/2} - \ {}_0^C D_t^\gamma \rho^{j-1/2} + \ {}_0^C D_t^\gamma \rho^{j-1/2}\|_0^2 \\ &\le C\Big(\|\overline{\nabla}_t^\gamma \rho^{j-1/2} - \ {}_0^C D_t^\gamma \rho^{j-1/2}\|_0^2 + \|\ {}_0^C D_t^\gamma \rho^{j-1/2}\|_0^2\Big) \\ &\le C\tau^{2(3-\gamma)} \max_{0\le t\le T}\|\rho_{ttt}^{j-1/2}\|_0^2 + C\|\ {}_0^C D_t^\gamma \rho^{j-1/2}\|_0^2 \\ &\le C\tau^{2(3-\gamma)} + Ch^{2\mu-2\lambda}\|\ {}_0^C D_t^\gamma u^{j-1/2}\|_{H^\mu(\Omega)}^2.\end{aligned} \tag{5.40}$$

Therefore, by inequalities (5.39)-(5.40), we have

$$\|\overline{R}_j\|_0^2 \le C\tau^{2(3-\gamma)} + Ch^{2\mu-2\lambda}\|\ {}_0^C D_t^\gamma u^{j-1/2}\|_{H^\mu(\Omega)}^2. \tag{5.41}$$

Inserting inequalities (5.37), (5.38) and (5.41) into the estimate (5.36), then we obtain

$$\begin{aligned}\|\theta^n\|_{(\alpha,\beta)}^2 \le& C\|u_h^0 - u^0\|_{(\alpha,\beta)}^2 + Ch^{2\mu-2\lambda}\|u^0\|_{H^\mu(\Omega)}^2 \\ &+ C\Big(\|(u_h^0)_t - u_t^0\|_0^2 + h^{2\mu-2\lambda}\|u_t^0\|_{H^\mu(\Omega)}^2\Big) \\ &+ C\max_{1\le j\le n}\Big\{\tau^{2(3-\gamma)} + h^{2\mu-2\lambda}\|\ {}_0^C D_t^\gamma u^{j-1/2}\|_{H^\mu(\Omega)}^2\Big\}.\end{aligned} \tag{5.42}$$

Since $u_h^n - u^n = e^n = \rho^n + \theta^n$,

$$\|\rho^n\|_{(\alpha,\beta)}^2 = \|P_h u^n - u^n\|_{(\alpha,\beta)}^2 \le Ch^{2\mu-2\lambda}\|u^n\|_{H^\mu(\Omega)}^2, \tag{5.43}$$

and hence

$$\begin{aligned}\|u_h^n - u^n\|_{(\alpha,\beta)}^2 &\le C(\|\rho^n\|_{(\alpha,\beta)}^2 + \|\theta^n\|_{(\alpha,\beta)}^2)\\ &\le Ch^{2\mu-2\lambda}\|u^n\|_{H^\mu(\Omega)}^2 + C\|u_h^0 - u^0\|_{(\alpha,\beta)}^2 + Ch^{2\mu-2\lambda}\|u^0\|_{H^\mu(\Omega)}^2\\ &+ C\|(u_h^0)_t - u_t^0\|_0^2 + Ch^{2\mu-2\lambda}\|u_t^0\|_{H^\mu(\Omega)}^2\\ &+ C\Big\{\tau^{2(3-\gamma)} + h^{2\mu-2\lambda}\max_{1\le j\le n}\|\,{}_0^C D_t^\gamma u^{j-1/2}\|_{H^\mu(\Omega)}^2\Big\}.\end{aligned} \tag{5.44}$$

When choosing the interpolations as initial values of u and u_t at time t_0, i.e. $u_h^0 = \Pi_h u^0$, $(u_h^0)_t = \Pi_h u_t^0$, then by (5.20) we have

$$\begin{aligned}\|u_h^n - u^n\|_{(\alpha,\beta)}^2 &\le Ch^{2\mu-2\lambda}(\|u^n\|_{H^\mu(\Omega)}^2 + \|u^0\|_{H^\mu(\Omega)}^2 + \|u_t^0\|_{H^\mu(\Omega)}^2)\\ &+ C\Big\{\tau^{2(3-\gamma)} + h^{2\mu-2\lambda}\max_{1\le j\le n}\|\,{}_0^C D_t^\gamma u^{j-1/2}\|_{H^\mu(\Omega)}^2\Big\}.\end{aligned} \tag{5.45}$$

Then the convergence analysis is completed. □

6. **Numerical examples**

In this section, the unstructured mesh Crank-Nicolson Galerkin method is tested using linear triangular elements. By Theorem 5.2, we expect that $\|u_h^n - u(t_n)\|_0 \sim O(\tau^{3-\gamma} + h^2)$, $\|u_h^n - u(t_n)\|_{(\alpha,\beta)} \sim O(\tau^{3-\gamma} + h^{2-\lambda})$, where $\lambda = \max\{\alpha, \beta\}$, $\lambda < \mu \le s + 1$. To assess the overall performance of the proposed method, we give two numerical examples defined on the domain $\Omega = [0,1] \times [0,1]$ and the elliptical domain $\Omega = \{(x,y)|\frac{x^2}{a^2} + \frac{y^2}{b^2} < 1\}$, respectively. The number of the Gauss points in a certain triangular element E is taken as N_g^2. To illustrate the ability of the unstructured mesh formulation outlined in Section 4, a comparison of the accuracy and the computational cost between the structured and unstructured mesh for the same problem is conducted. The meshes are generated by the software Gmsh [14].

6.1. **Example 1.** Consider the following problem

$$\begin{cases} {}_0^C D_t^\gamma u = K_x \frac{\partial^{2\alpha} u}{\partial |x|^{2\alpha}} + K_y \frac{\partial^{2\beta} u}{\partial |y|^{2\beta}} + f(x,y,t), \quad (x,y,t) \in \Omega \times (0,T],\\ u(x,y,0) = 0, \quad (x,y) \in \Omega,\\ u_t(x,y,0) = 0, \quad (x,y) \in \Omega,\\ u(x,y,t) = 0, \quad (x,y,t) \in \partial\Omega \times (0,T], \end{cases} \tag{6.1}$$

TABLE 6.1. The computation times and the corresponding errors for the structured mesh and the unstructured mesh with $h \approx 1/8$, $\alpha = 0.8$, $\beta = 0.8$, $\gamma = 1.6$.

Gauss points (N_g^2)	meshes	$\|u_h^N - u(t_N)\|_0$	$\|u_h^N - u(t_N)\|_{(\alpha,\beta)}$	time(s)
$N_g = 1$	structured	1.1875e-4	8.4404e-4	15.4818
	unstructured	8.4824e-5	6.1325e-4	24.9804
$N_g = 2$	structured	6.1607e-5	1.0193e-3	54.7318
	unstructured	4.3817e-5	7.8474e-4	87.4780

where $1 < \gamma < 2$, $1/2 < \alpha, \beta < 1$, $K_x = K_y = 1$. The domain Ω is assumed to be $\Omega = [0,1] \times [0,1]$. The function $f(x,y,t)$ is

$$\begin{aligned} & f(x,y,t) \\ &= \frac{2t^{2-\gamma}}{\Gamma(3-\gamma)} x^2(1-x)^2 y^2(1-y)^2 + C_y \frac{1}{\Gamma(3-2\alpha)} [x^{2-2\alpha} + (1-x)^{2-2\alpha}] \\ &- C_y \frac{6}{\Gamma(4-2\alpha)} [x^{3-2\alpha} + (1-x)^{3-2\alpha}] + C_y \frac{12}{\Gamma(5-2\alpha)} [x^{4-2\alpha} + (1-x)^{4-2\alpha}] \\ &+ C_x \frac{1}{\Gamma(3-2\beta)} [y^{2-2\beta} + (1-y)^{2-2\beta}] - C_x \frac{6}{\Gamma(4-2\beta)} [y^{3-2\beta} + (1-y)^{3-2\beta}] \\ &+ C_x \frac{12}{\Gamma(5-2\beta)} [y^{4-2\beta} + (1-y)^{4-2\beta}], \end{aligned} \tag{6.2}$$

where $C_x = \frac{t^2 x^2 (1-x)^2}{\cos(\beta\pi)}$, $C_y = \frac{t^2 y^2 (1-y)^2}{\cos(\alpha\pi)}$. The exact solution is $u(x,y,t) = t^2 x^2 (1-x)^2 y^2 (1-y)^2$.

To clarify the ability of the unstructured mesh compared with the structured mesh in the implementation of the numerical scheme, the computational costs and the corresponding errors of the two kinds of partition for $T = 1$ are studied. To show the differences, we take the cases with $h \approx 1/8$ and $h \approx 1/16$ as examples. The meshes used for $\Omega = [0,1] \times [0,1]$ are shown in Fig. 6.1.

With parameters assumed to be $\alpha = 0.8$, $\beta = 0.8$, $\gamma = 1.6$, Table 6.1 and Table 6.2 present the computation times and the corresponding errors for the structured and unstructured meshes with $h \approx 1/8$ and $h \approx 1/16$, respectively. An immediate observation from Table 6.1 and Table 6.2, for both the structured and the unstructured partitions, is that the computation times for the cases with $h \approx 1/16$ are distinct much longer than that for the cases with $h \approx 1/8$. Also for a certain h, the unstructured mesh requires a longer computation time compared with the structured

TABLE 6.2. The computation times and the corresponding errors for the unstructured mesh and the structured mesh with $h \approx 1/16$, $\alpha = 0.8$, $\beta = 0.8$, $\gamma = 1.6$.

Gauss points (N_g^2)	meshes	$\|u_h^N - u(t_N)\|_0$	$\|u_h^N - u(t_N)\|_{(\alpha,\beta)}$	time(s)
$N_g = 1$	structured	3.0455e-5	3.4951e-4	189.7850
	unstructured	2.4247e-5	2.6063e-4	289.2325
$N_g = 2$	structured	1.4295e-5	4.4551e-4	634.0120
	unstructured	1.0751e-5	3.5597e-4	998.1467

TABLE 6.3. Errors and convergence orders of the CNGM for Example 1 with $\tau = 1/2000$, $N_g = 2$.

	h	$\|u_h^N - u(t_N)\|_0$	order	$\|u_h^N - u(t_N)\|_{(\alpha,\beta)}$	order
	1/4	1.7830e-4		1.8402e-3	
$\gamma = 1.6$	1/8	4.3817e-5	2.0248	7.8474e-4	1.2296
$\alpha = 0.8$	1/16	1.0751e-5	2.0271	3.5597e-4	1.1404
$\beta = 0.8$	1/24	4.6863e-6	2.0479	2.1909e-4	1.1971
	1/32	2.5419e-6	2.1264	1.5766e-4	1.1439
	1/4	1.7679e-4		1.1925e-3	
$\gamma = 1.3$	1/8	4.3331e-5	2.0286	4.5683e-4	1.3843
$\alpha = 0.7$	1/16	1.0959e-5	1.9833	1.8633e-4	1.2938
$\beta = 0.6$	1/24	5.0812e-6	1.8957	1.1225e-4	1.2501
	1/32	2.9345e-6	1.9084	77553e-5	1.2852

TABLE 6.4. Errors and convergence orders of the CNGM for Example 1 with $\tau = 1/2000$, $N_g = 2$.

	h	$\|u_h^N - u(t_N)\|_0$	order	$\|u_h^N - u(t_N)\|_{(\alpha,\beta)}$	order
	1/4	1.7938e-4		1.7078e-3	
$\gamma = 1.5$	1/8	4.7596e-5	1.9141	7.1453e-4	1.2571
$\alpha = 0.6$	1/16	1.2119e-5	1.9736	3.2985e-4	1.1152
$\beta = 0.85$	1/24	5.4457e-6	1.9729	2.0664e-4	1.1535
	1/32	2.9609e-6	2.1181	1.5067e-4	1.0980
	1/4	1.7607e-4		1.5657e-3	
$\gamma = 1.3$	1/8	4.4268e-5	1.9918	6.3404e-4	1.3042
$\alpha = 0.65$	1/16	1.0987e-5	2.0105	2.7995e-4	1.1794
$\beta = 0.8$	1/24	4.8568e-6	2.0134	1.7074e-4	1.2195
	1/32	2.6718e-6	2.0774	1.2211e-4	1.1653

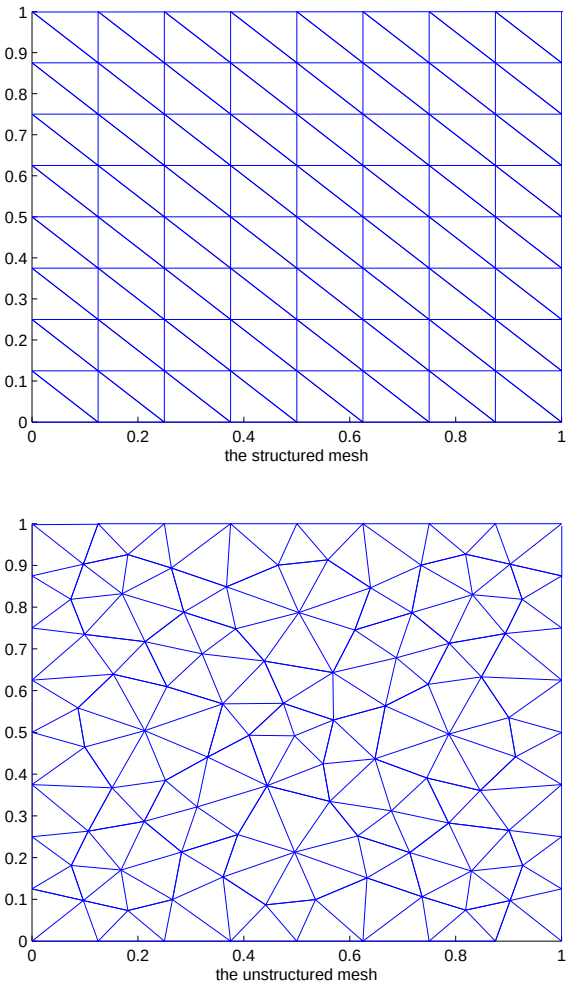

FIGURE 6.1. The structured mesh and the unstructured mesh for $\Omega = [0,1] \times [0,1]$ with $h \approx 1/8$.

.

mesh. In fact, the computational cost depends on the number of nodes and elements in the partition. For the case of the structured meshes, there are 81 nodes and 128 elements in the partition with $h \approx 1/8$, and there are 289 nodes and 512 elements in the partition with $h \approx 1/16$. For the case of the unstructured meshes, there are 109 nodes and 184 elements in the partition with $h \approx 1/8$, and there are 371 nodes and 676 elements in the partition with $h \approx 1/16$. A smaller h will lead to more nodes and

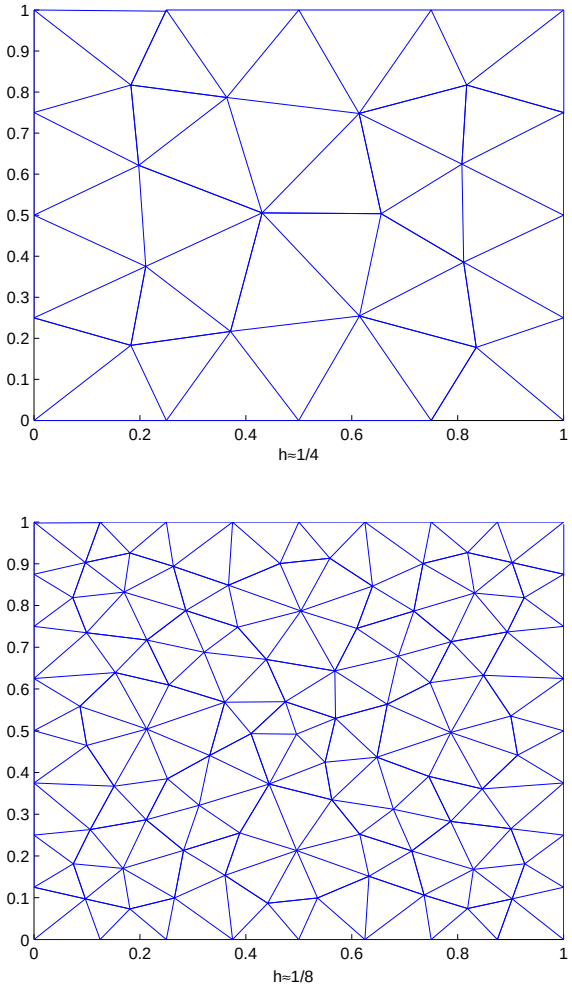

FIGURE 6.2. The unstructured meshes for $\Omega = [0,1] \times [0,1]$ with $h \approx 1/4$ and $h \approx 1/8$.

.

elements, and more Gauss points needed to be calculated. As a result, a denser partition will require a larger computational cost. Furthermore, for a certain h, more elements result in more Gauss points needed to be handled in the unstructured mesh, which accounts for the larger computational cost required for the unstructured mesh compared with the structured mesh.

On the other hand, in each case, the errors for the unstructured meshes are shown to be smaller than that for the structured meshes in both the

$\|\cdot\|_0$ norm and the $\|\cdot\|_{(\alpha,\beta)}$ norm. Note that for a certain h, there are more nodes and elements in the unstructured mesh than the structured mesh. It is demonstrated that a denser partition will lead to a better performance of the numerical scheme, that is also in accordance with the fact presented in Table 6.1 and Table 6.2. Therefore, for the proposed Galerkin method using an unstructured mesh, compared with the existing method using a structured mesh, the computational cost increases to some extent but the precision of the scheme is improved.

The number of Gauss points in a certain triangular element appears better for $N_g = 2$, with smaller errors for both the meshes observed. In view of this, to verify the theoretical analysis of the novel unstructured mesh CNGM, we choose $N_g = 2$, which means there are four Gauss points in each triangular element in the mesh. The domain Ω is partitioned by the unstructured meshes as shown in Fig. 6.2.

For time $T = 1$, the errors and convergence orders for different values of α, β, γ in the spatial direction by the $\|\cdot\|_0$ norm and the $\|\cdot\|_{(\alpha,\beta)}$ norm are presented in Table 6.3 and Table 6.4 with $\tau = 1/2000$, respectively. From Table 6.3 and Table 6.4, for arbitrary values of α, β, γ, the convergence orders in the $\|\cdot\|_0$ norm approximate 2 and the convergence orders in the $\|\cdot\|_{(\alpha,\beta)}$ norm approximate $2 - \max\{\alpha, \beta\}$, which are consistent with the theoretical analysis presented in Section 5. It is demonstrated that the unstructured mesh Crank-Nicolson Galerkin method works well in solving the two-dimensional time-space fractional wave equation.

6.2. **Example 2.** In this example, we consider a two-dimensional time-space fractional wave equation defined on an elliptical domain Ω, where $\Omega = \{(x, y) | \frac{x^2}{a^2} + \frac{y^2}{b^2} < 1\}$.

$$\begin{cases} {}_0^C D_t^\gamma u = K_x \frac{\partial^{2\alpha} u}{\partial |x|^{2\alpha}} + K_y \frac{\partial^{2\beta} u}{\partial |y|^{2\beta}} + f(x, y, t), \quad (x, y, t) \in \Omega \times (0, T], \\ u(x, y, 0) = \phi(x, y), \quad (x, y) \in \Omega, \\ u_t(x, y, 0) = 0, \quad (x, y) \in \Omega, \\ u(x, y, t) = 0, \quad (x, y, t) \in \partial\Omega \times (0, T], \end{cases} \tag{6.3}$$

where $1<\gamma<2$, $1/2<\alpha,\beta<1$, $\phi(x,y)=(\frac{x^2}{a^2}+\frac{y^2}{b^2}-1)^2$, and

$$
\begin{aligned}
&f(x,y,t)\\
&=\frac{2t^{2-\gamma}}{\Gamma(3-\gamma)}(\frac{x^2}{a^2}+\frac{y^2}{b^2}-1)^2+C_x\frac{\Gamma(5)(x-x_l)^{4-2\alpha}}{a^4\Gamma(5-2\alpha)}+C_x\frac{4x_l\Gamma(4)(x-x_l)^{3-2\alpha}}{a^4\Gamma(4-2\alpha)}\\
&+C_x(\frac{6x_l^2}{a^4}+\frac{2y^2}{a^2b^2}-\frac{2}{a^2})\frac{\Gamma(3)(x-x_l)^{2-2\alpha}}{\Gamma(3-2\alpha)}+C_x\frac{\Gamma(5)(x_r-x)^{4-2\alpha}}{a^4\Gamma(5-2\alpha)}\\
&-C_x\frac{4x_r\Gamma(4)(x_r-x)^{3-2\alpha}}{a^4\Gamma(4-2\alpha)}+C_x(\frac{6x_r^2}{a^4}+\frac{2y^2}{a^2b^2}-\frac{2}{a^2})\frac{\Gamma(3)(x_r-x)^{2-2\alpha}}{\Gamma(3-2\alpha)}\\
&+C_y\frac{\Gamma(5)(y-y_l)^{4-2\beta}}{b^4\Gamma(5-2\beta)}+C_y\frac{4y_l\Gamma(4)(y-y_l)^{3-2\beta}}{b^4\Gamma(4-2\beta)}\\
&+C_y(\frac{6y_l^2}{b^4}+\frac{2x^2}{a^2b^2}-\frac{2}{b^2})\frac{\Gamma(3)(y-y_l)^{2-2\beta}}{\Gamma(3-2\beta)}+C_y\frac{\Gamma(5)(y_r-y)^{4-2\beta}}{b^4\Gamma(5-2\beta)}\\
&-C_y\frac{4y_r\Gamma(4)(y_r-y)^{3-2\beta}}{b^4\Gamma(4-2\beta)}+C_y(\frac{6y_r^2}{b^4}+\frac{2x^2}{a^2b^2}-\frac{2}{b^2})\frac{\Gamma(3)(y_r-y)^{2-2\beta}}{\Gamma(3-2\beta)},
\end{aligned}
\tag{6.4}
$$

where $C_x=\frac{K_x(t^2+1)}{2\cos(\alpha\pi)}$, $C_y=\frac{K_y(t^2+1)}{2\cos(\beta\pi)}$, $x_l=-\frac{a}{b}\sqrt{b^2-y^2}, x_r=\frac{a}{b}\sqrt{b^2-y^2}$, $y_l=-\frac{b}{a}\sqrt{a^2-x^2}, y_r=\frac{b}{a}\sqrt{a^2-x^2}$. The exact solution is $u(x,y,t)=(t^2+1)(\frac{x^2}{a^2}+\frac{y^2}{b^2}-1)^2$.

We assume $K_x=2, K_y=1, a=1/2, b=1/4$, $T=1$. Fig. 6.3 shows the unstructured meshes for the convex elliptical domain with $h\approx 1/16$ and $h\approx 1/32$. For different values of α,β,γ, the errors and convergence orders in the spatial direction by the $\|\cdot\|_0$ norm and the $\|\cdot\|_{(\alpha,\beta)}$ norm are presented in Table 6.5 and Table 6.6 with $\tau=1/3200$, respectively.

Tables 6.5 and 6.6 show that for arbitrary values of α,β,γ, the convergence orders in the $\|\cdot\|_0$ norm approximate 2 and the convergence orders in the $\|\cdot\|_{(\alpha,\beta)}$ norm approximate $2-\max\{\alpha,\beta\}$. In other words, the convergence orders in both the L^2-norm and the $\|\cdot\|_{(\alpha,\beta)}$ norm are in accordance with the theoretical analysis, indicating that the Crank-Nicolson Galerkin method is efficient in dealing with the two-dimensional time-space fractional wave equation on a convex domain.

Note that the convex elliptical domain is difficult to partition with a structured mesh, the existing finite element method using the structured meshes is less efficient. In many practical applications, the solution domain tends to be irregular, such as the human brain or heart, and for such applications, the proposed numerical method using an unstructured mesh will be more effective and feasible. Furthermore, the structured mesh can be treated as a special case of the unstructured mesh, but not vice versa.

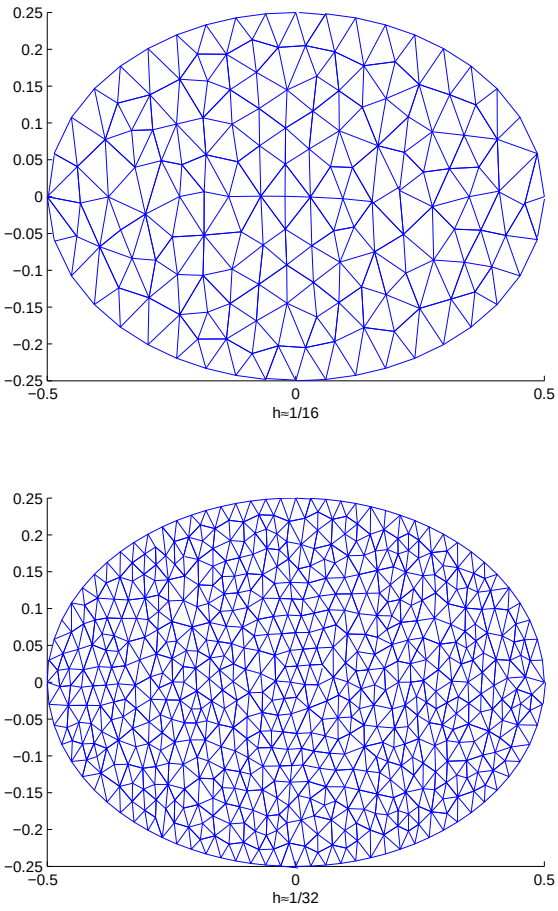

FIGURE 6.3. The unstructured meshes for elliptical domain with $h \approx 1/16$ and $h \approx 1/32$

.

7. **Conclusions**

In this paper, a novel unstructured mesh finite element method is developed for solving the two-dimensional time-space fractional wave equation on an irregular convex domain. The Crank-Nicolson scheme is used to discretize the Caputo time frational derivative, and to discretize in space, the novel Galerkin finite element method using a completely unstructured mesh is applied. Then the implementation of the unstructured mesh Crank-Nicolson Galerkin method is detailed and the stability and convergence of

TABLE 6.5. Errors and convergence orders of the CNGM for Example 2 with $\tau = 1/3200$, $N_g = 2$.

	h	$\|u_h^N - u(t_N)\|_0$	order	$\|u_h^N - u(t_N)\|_{(\alpha,\beta)}$	order
	1/8	4.4247e-2		8.4576e-1	
$\gamma = 1.6$	1/16	1.1467e-2	1.9481	3.9559e-1	1.0962
$\alpha = 0.8$	1/22	6.1807e-3	1.9408	2.6931e-1	1.2075
$\beta = 0.8$	1/32	3.0282e-3	1.9042	1.7801e-1	1.1049
	1/48	1.3708e-3	1.9548	1.1002e-1	1.1869
	1/8	4.4985e-2		4.6146e-1	
$\gamma = 1.3$	1/16	1.2109e-2	1.8934	1.9770e-1	1.2229
$\alpha = 0.7$	1/22	6.5675e-3	1.9211	1.2800e-1	1.3651
$\beta = 0.6$	1/32	3.2885e-3	1.8461	8.2263e-2	1.1799
	1/48	1.5239e-3	1.8969	4.9411e-2	1.2572

TABLE 6.6. Errors and convergence orders of the CNGM for Example 2 with $\tau = 1/3200$, $N_g = 2$.

	h	$\|u_h^N - u(t_N)\|_0$	order	$\|u_h^N - u(t_N)\|_{(\alpha,\beta)}$	order
	1/8	4.3560e-2		8.8461e-1	
$\gamma = 1.5$	1/16	1.1197e-2	1.9599	4.473e-1	1.0929
$\alpha = 0.6$	1/22	5.8478e-3	2.0398	2.8420e-1	1.1868
$\beta = 0.85$	1/32	2.7473e-3	2.0162	1.8481e-1	1.1486
	1/48	1.2150e-3	2.0121	1.1609e-1	1.1468
	1/8	4.3002e-2		5.6047e-1	
$\gamma = 1.6$	1/16	1.0981e-2	1.9694	2.3503e-1	1.2538
$\alpha = 0.65$	1/22	5.7921e-3	2.0086	1.5239e-1	1.3604
$\beta = 0.7$	1/32	2.7611e-3	1.9773	9.5672e-2	1.2425
	1/48	1.2513e-3	1.9520	5.7342e-2	1.2625

the numerical scheme are analysed. Finally, some numerical examples are given to verify the theoretical analysis. The results show that the unstructured mesh Crank-Nicolson Galerkin method works well in dealing with the two-dimensional time-space fractional wave equation on an irregular convex domain. Furthermore, by the comparison of the unstructured mesh with the structured mesh in the implementation of the numerical scheme, the proposed unstructured mesh finite element method is shown to require a larger computational cost but leads to a better performance with smaller errors of the numerical scheme compared with the existing finite element method using the structured meshes. Given that many practical problems

involve irregular convex domains, which are difficult to partition well with a structured mesh, research on the finite element method using a completely unstructured mesh is of great significance. More complex convex domains and more general initial and boundary conditions will be considered in future work.

Acknowledgements

This work was supported by the National Natural Science Foundation of China (Grants 11472161 and 91130017), the Independent Innovation Foundation of Shandong University (Grant 2013ZRYQ002), and the Natural Science Foundation of Shandong Province (Grant ZR2014AQ015), the Australian Research Council Grant DP150103675, and the State Scholarship Fund from China Scholarship Council. The authors would like to express their sincere thanks to the anonymous referees for their constructive comments and suggestions to improve the quality of the paper.

References

[1] E. Bazhlekova, I. Bazhlekov, Viscoelastic flows with fractional derivative models: Computational approach by convolutional calculus of Dimovski. *Fract. Calc. Appl. Anal.*, **17**, No 4 (2014), 954-976.

[2] W. Bu, X. Liu, Y. Tang, J. Yang, Finite element multigrid method for multi-term time fractional advection diffusion equations. *Int. J. Model. Simul. Sci. Comput.* **6**, No 1 (2015) 1540001.

[3] W. Bu, Y. Tang, Y. Wu, J. Yang, Finite difference/finite element method for two-dimensional space and time fractional Bloch-Torrey equations. *J. Comput. Phys.* **293**, (2015), 264-279.

[4] W. Bu, Y. Tang, J. Yang, Galerkin finite element method for two-dimensional Riesz space fractional diffusion equations. *J. Comput. Phys.* **276**, (2014), 26-38.

[5] S. Chen, F. Liu, X. Jiang, I. Turner, K. Burrage, Fast Finite Difference Approximation for Identifying Parameters in a Two-dimensional Space-fractional Nonlocal Model with Variable Diffusivit Coefficients. *SIAM J. Numer. Anal.* **54**, No 2 (2016), 606-624.

[6] Y. J. Choi, S.K. Chung, Finite element solutions for the space fractional diffusion equation with a nonlinear source term. In *Abstr. Appl. Anal.* volume 2012. Hindawi Publishing Corporation, (2012).

[7] G. R. Cowper, Gaussian quadrature formulas for triangles. *Int. J. Numer. Meth. Eng.* **7**, No 3 (1973), 405-408.

[8] M. Cristescu, G. Loubignac, *Gaussian Quadrature Formulas for Functions with Singularities in* $1/R$ *over Triangles and Quadrangles*. Pentech Press, London, UK, (1978).

[9] V. J. Ervin, J. P. Roop, Variational formulation for the stationary fractional advection dispersion equation. *Numer. Meth. Part. D. E.* **22**, No 3 (2006), 558-576.

[10] V. J. Ervin, J. P. Roop, Variational solution of fractional advection dispersion equations on bounded domains in R^d. *Numer. Meth. Part. D. E.* **23**, (2007), 256-281.

[11] W. Fan, X. Jiang, S. Chen, Parameter estimation for the fractional fractal diffusion model based on its numerical solution. *Comput. Math. Appl.* **71**, No 2 (2016), 642-651.

[12] L. Feng, P. Zhuang, F. Liu, I. Turner, Stability and convergence of a new finite volume method for a two-sided space-fractional diffusion equation. *Appl. Math. Comput.* **257**, (2015),52-65.

[13] N. Ford, J. Xiao, Y. Yan, A finite element method for time fractional partial differential equations. *Fract. Calc. Appl. Anal.* **14**, No 3 (2011), 454-474.

[14] C. Geuzaine J. F. Remacle, Gmsh: A 3-D finite element mesh generator with built-in pre-and post-processing facilities. *Int. J. Numer. Meth. Eng.* **79**, No 11 (2009), 1309-1331.

[15] C. Gong, W. Bao, G. Tang, A parallel algorithm for the Riesz fractional reaction-diffusion equation with explicit finite difference method. *Fract. Calc. Appl. Anal.* **16**, No 3 (2013), 654-669.

[16] H. Hejazi, T. Moroney, F. Liu, Stability and convergence of a finite volume method for the space fractional advection-dispersion equation. *J. Comput. Appl. Math.* **255**, (2014), 684-697.

[17] R. Hilfer, *Applications of Fractional Calculus in Physics*. World Scientific, (2000).

[18] X. Jiang, H. Qi, Thermal wave model of bioheat transfer with modified Riemann-Liouville fractional derivative. *J. Phys. A: Math. Theor.* **45**, No 48 (2012), 485101.

[19] C. Li, Z. Zhao, Y. Chen, Numerical approximation of nonlinear fractional differential equations with subdiffusion and superdiffusion. *Comput. Math. Appl.* **62** No 3 (2011), 855-875.

[20] F. Liu, P. Zhuang, Q. Liu, *Numerical Methods of Fractional Partial Differential Equations and Applications*. Science Press, Beijing, China, (2015) (In Chinese).

[21] L. Liu, L. Zheng, F. Liu, X. Zhang, Anomalous convection diffusion and wave coupling transport of cells on comb frame with fractional Cattaneo-Christov flux. *Commun. Nonlinear Sci.* **38**, (2016), 45-58.

[22] I. Podlubny, *Fractional Differential Equations: An Introduction to Fractional Derivatives, Fractional Differential Equations, to Methods*

of their Solution and some of their Applications, volume 198. Academic Press, (1998).

[23] J. P. Roop, Variational solution of the fractional advection dispersion equation. *Ph.D. thesis*, (2004).

[24] Z. Sun, X. Wu, A fully discrete difference scheme for a diffusion-wave system. *Appl. Numer. Math.* **56**, No (2) (2006), 193-209.

[25] B. Yu, X. Jiang, H. Xu, A novel compact numerical method for solving the two-dimensional non-linear fractional reaction-subdiffusion equation. *Numer. Algorithms* **68**, No 4 (2015), 923-950.

[26] F. Zeng, F. Liu, C. Li, K. Burrage, I. Turner, V. Anh, A Crank-Nicolson ADI spectral method for a two-dimensional Riesz space fractional nonlinear reaction-diffusion equation. *SIAM J. Numer. Anal.* **52**, No 6 (2014), 2599-2622.

[27] H. Zhang, F. Liu, V. Anh, Galerkin finite element approximation of symmetric space-fractional partial differential equations. *Appl. Math. Comput.* **217**, No 6 (2010), 2534-2545.

[28] Y. Zhao, W. Bu, J. Huang, D. Liu, Y. Tang, Finite element method for two-dimensional space-fractional advection-dispersion equations. *App. Math. Comput.* **257**, (2015), 553-565.

[29] Y. Zhao, Y. Zhang, D. Shi, F. Liu, I. Turner, Superconvergence analysis of nonconforming finite element method for two-dimensional time fractional diffusion equations. *Appl. Math. Lett.* **59**, (2016), 38-47.

[30] M. Zheng, F. Liu, V. Anh, I. Turner, A high-order spectral method for the multi-term time-fractional diffusion equations. *Appl. Math. Model.* **40**, No 7 (2016), 4970-4985.

[31] X. Zhu, Y. Nie, J. Wang, Z. Yuan, A numerical approach for the Riesz space-fractional Fisher' equation in two-dimensions. *Int. J. Comput. Math.* (2015), 1-20.

[32] P. Zhuang, F. Liu, I. Turner, Y. Gu, Finite volume and finite element methods for solving a one-dimensional space-fractional Boussinesq equation. *Appl. Math. Model.* **38**, No 15 (2014), 3860-3870.

[1] *School of Mathematics, Shandong University*
Jinan 250100, PR China

e-mail: wenping0218@126.com
[2] *Corresponding author.*
School of Mathematical Sciences, Queensland University of Technology
GPO Box 2434, Brisbane, QLD 4001, Australia

e-mail: f.liu@qut.edu.au
[3] *Corresponding author.*
School of Mathematics, Shandong University

Jinan 250100, PR China

e-mail: wqjxyf@sdu.edu.cn

[4] *ACEMS ARC Centre of Excellence,*
School of Mathematical Sciences, Queensland University of Technology
GPO Box 2434, Brisbane, QLD 4001, Australia

e-mail: i.turner@qut.edu.au